Subcellular localization of nucleocapsid protein of severe fever with thrombocytopenia syndrome virus (SFTSV) and characterization of quasi-species of SFTSV
（重症熱性血小板減少症候群ウイルス(SFTSV)の核蛋白の細胞内局在および SFTSV の多種性の解析）

Lokupathirage Sithumini Madubashini Wimalasiri

Dedication

Every challenging work needs self-efforts and the support, love, and encouragement of loved ones, especially those very close to our hearts.
I dedicate my humble effort to my sweet and loving husband, *Sampath Miriyagalla*, and my daughter, *Oneli Nathasha Miriyagalla.*

This work is also dedicated to my parents, *L D Wimalasiri* and *M P N Damayanthi*, who has always loved me unconditionally and whose good examples have taught me to work hard for the things I aspire to achieve.

The dedication also goes to the memory of my grandparents, *M. John Singho* and *S. Weerasooriya*, for being my first educators, mentors, and role models.

Table of contents

Table of figures and tables

Abbreviations

BHK	Baby hamster kidney
BSA	Bovine serum albumin
BSL	Biosafety level
CPE	Cytopathic effect
DAPI	4′,6-diamidino-2-phenylindole
DMEM	Dulbecco’s modified Eagle’s medium
DMSO	Dimethyl sulfoxide
DNA	Deoxyribonucleic acid
dpi	Days post infection
eGFP	Enhanced green fluorescent protein
EMEM	Eagle’s minimum essential medium
ER	Endoplasmic reticulum
ERGIC	ER-Golgi intermediate compartment
FBS	Fetal bovine serum
Fluc	Firefly luciferase
GAPDH	Glyceraldehyde 3-phosphate dehydrogenase
GP	Glycoprotein
GPC	Glycoprotein precursor
HA	Hemagglutinin
HEK	Human embryonic kidney
HRP	Horseradish peroxidase
IFA	Immunofluorescent antibody assay
IgG	Immunoglobulin G
IL	Interleukin

IP	Immunoprecipitation
L	Large
M	Medium
mAb	Monoclonal antibody
MCC	Mander's correlation coefficient
MOI	Multiplicity of infection
NMMHC-IIA	Nonmuscle myosin heavy chain IIA
NLRP3	NOD-like receptor protein 3
NSs	Non-structural protein
NP	Nucleoprotein
pAb	Polyclonal antibody
PAGE	Polyacrylamide gel electrophoresis
PARP	Poly ADP-ribose polymerase
PBS	Phosphate buffered saline
PCC	Pearson's correlation coefficient
PCR	Polymerase chain reaction
PFU	Plaque-forming units
PPBS	Paraformaldehyde phosphate buffer solution
PVDF	Polyvinylidene difluoride
qPCR	Quantitative PCR
RdRp	RNA-dependent RNA polymerase
RLU	Renilla Luciferase units
Rluc	Renilla luciferase
RNA	Ribonucleic acid
RNP	Ribonucleoprotein complex

RT-PCR	Reverse-transcription polymerase chain reaction
RVFV	Rift Valley fever virus
S	Small
SDS	Sodium dodecyl sulfate
SFTS	Severe fever with thrombocytopenia syndrome
SFTSV	Severe fever with thrombocytopenia syndrome virus
TPB	Tryptose phosphate broth
vRNA	Viral genomic RNA
VSV	Vesicular stomatitis virus
YG	Yamaguchi

Notes

This thesis contains two chapters, and the first chapter has been published as follows.

- Lokupathirage, S. M. W., Tsuda, Y., Ikegame, K., Noda, K., Muthusinghe, D. S., Kozawa, F., Manzoor, R., Shimizu, K.,Yoshimatsu, K. (2021). Subcellular localization of nucleocapsid protein of SFTSV and its assembly into the ribonucleoprotein complex with L protein and viral RNA. Sci Rep, 11(1), 22977. doi:10.1038/s41598-021-01985-x

Preface

Severe fever with thrombocytopenia syndrome (SFTS) is an emerging zoonotic disease caused by the SFTS virus (SFTSV), a member of the genus *Bandavirus*, family *Phenuiviridae* and the order *Bunyavirales*. The SFTS is widely distributed in East Asian countries, including China, Japan, South Korea, Vietnam, Taiwan, Myanmar, and Thailand. The mortality rate of SFTS reaches up to 35% in Japan[1], where it becomes a public health concern. The Asian long-horned ticks, *Haemaphysalis longicornis*, are the main transmission vector of SFTSV[2]. The affected population of SFTS is elderly farmers working in the fields and veterinarians, people with close contact with animals showing animal-to-human transmission. Person-to-person transmission through infected body fluids of SFTSV and nosocomial infection also has been reported[3]. The main clinical symptoms of SFTS are thrombocytopenia, leucopenia, acute fever, hemorrhage, and gastrointestinal symptoms. These were generally reported at the onset of the disease[4]. The disease typically has four stages: incubation, fever , multiple organ failure, and convalescence. The SFTSV YG1 strain was isolated from the first SFTSV patient in Yamaguchi (YG) prefecture in Japan[5]. This strain was used in the experiments reported in this thesis.

SFTSV consists of three negative-sense RNA segments designated as small (S), medium (M), and large (L); the S segment encodes nucleoprotein (N) and non-structural protein (NSs), the M segment encodes the glycoproteins precursor (GPC) that cleaved to two envelope glycoproteins (GPs), Gn and Gc, whereas; the L segment encodes an RNA-dependent RNA polymerase (RdRp) also called as L protein[6].

The N is responsible for the genomic RNA packaging, replication, transcription, assembly and encapsulating into the ribonucleoprotein complex (RNP: a complex of N, RdRp, and viral genome) as a protection mechanism of the immune system in the host cell. The GP takes part in cell entry to target cells and virus assembly. The L protein has vital roles in replication

and transcription. NSs have diverse functions related to the activity of viral polymerase, suppression of viral replication and blocking of interferon production through various mechanisms.

The replication of phenuiviruses begins with the attachment of GP to the cell membrane of host cells via the interaction of Gn and Gc with host cell receptors. The virus internalization occurs via receptor-mediated endocytosis followed by the acidification of endocytic vesicles, which leads to cell fusion of the viral membrane with the endosomal membrane.

Then, RNP is released into the cell cytoplasm and replicated and transcribed by RdRp. RdRp catalyzes the primary transcription of viral mRNAs, which are primed by host cell-derived primers. The three negative-sense viral genome segments are converted into positive-sense antigenomes for genome replication. In ribosomes, GPC is translated and then modified into GP by cleavage into Gn at N-terminus and Gc at the C-terminus. The GP traffics into the ER-Golgi intermediate compartment (ERGIC) and Golgi complex, whereas Nand RdRp are synthesized in the free ribosomes in the cell cytoplasm. The synthesized NP, RdRp, together with the viral genomic RNA(vRNA), form the RNPs in the cell cytoplasm and then are transported to membranes of the Golgi complex that have been modified by insertion of Gn and Gc. The virus particles bud into Golgi membrane-derived vesicles. Golgi vesicles that contain virus particles are trafficked to the cell surface, and the fusion of the vesicular membranes with the plasma membrane leads to the release of infectious virions by exocytosis.

Even though the SFTS has been investigated for over a decade in Japan and other East Asian countries, there are no effective measures to control the spread of the infection. SFTS cases in endemic regions has been reported and there are no effective antiviral drugs or vaccines. However, the molecular mechanism has yet to be elucidated entirely in SFTSV virion formation, which is vital to produce antivirals for the disease.

The viruses of the family *Phenuiviridae* show the fusion of Gc with the endosomal membrane under acidic conditions, followed by endocytosis[7,8]. The virus-mediated cell-cell fusion can merge the cell membrane and the cytoplasm to form multinucleated cells, called syncytia. Furthermore, the infected cells with the viruses of the family *Phenuiviridae* such as SFTSV and the Rift Valley fever virus (RVFV) can cause a cytopathic effect (CPE)[9,10].

Our previous studies have shown that SFTSV YG1 showed variety of virological properties in YG1 quasispecies, such as CPE-related cell death and cell fusion[9,11].This might be due to the mutations of each quasispecies. This thesis covers two topics divided into two chapters. Chapter 1 describes the subcellular localization of N and its assembly into the RNP complex with L protein and viral RNA . Chapter 2 focuses on developing recombinant viruses bearing single mutations to compare the unique virological characteristics of each mutation of the subclones of YG1. The virological characteristics: cell fusion, and CPE-related cell death were also assessed and compared among the quasispecies.

Chapter 1

Subcellular localization of nucleocapsid protein of SFTSV and its assembly into the ribonucleoprotein complex with L protein and viral RNA

Introduction

SFTS is an emerging zoonosis caused by the SFTSV, which belongs to the genus *Bandavirus* in the family *Phenuiviridae*, order *Bunyavirales* according to the International Committee on Taxonomy of Viruses classification criteria. SFTS was first reported in Hubei province in China in 2009; in Japan, it was first identified in Yamaguchi Prefecture in 2013[5,12]. SFTS patients have been reported in Korea and Vietnam, and SFTS is now considered as an infectious disease widely distributed in East Asia[13,14]. SFTS is a tick-borne zoonotic disease characterized by fever, gastrointestinal symptoms, thrombocytopenia, and leukopenia[15]. The fatality rate of SFTS in Japan is 6%–30%, while the fatality rate in other countries is 12%–47%[6,16,17]. Since effective drugs and vaccines have not yet been developed, it is essential to understand the viral replication mechanism to develop antiviral agents against SFTS.

The RNA genome of SFTSV is tripartite, negative or ambi-sense, single-stranded RNA designated as S, M, and L segments, which encode for the N protein and the NSs, GP, and L protein which has main role on RdRp activity, respectively. The bunyaviruses enter the cell by binding to receptors such as C-type lectin on dendritic cells via the GP, and then the virus is taken up into the cells by clathrin-dependent endocytosis[18,19]. As a result, the RNP complex is released into the cell cytoplasm, which causes transcription and replication of vRNA. In the cytoplasm, N protein and RdRp are expressed in the cytoplasm where they form the RNP complex with the vRNA[20]. Gn and Gc, which are translated in the endoplasmic reticulum (ER), associate with the RNP complex in the ERGIC or Golgi apparatus, followed by budding at the membranes of the Golgi apparatus[21,22]. Finally, Golgi vesicles containing virus particles are trafficked to the cell surface and release infectious virions extracellularly via exocytosis.

Ipreviously reported that SFTSV structural proteins were localized together in the ERGIC and Golgi apparatus in SFTSV-infected cells[22]. In cells transfected with all viral proteins, GP localized to the ER, ERGIC, and Golgi apparatus, but N protein or RdRp alone did not localize to any cellular compartment. In co-transfection experiments with GP, a small amount of RdRp, but not N protein, changed the localization of GP and move to the ERGIC and Golgi apparatus[22]. In this study, Iaimed to elucidate the mechanism of the localization of N protein to the ERGIC and Golgi apparatus, which is imperative for the replication cycle of SFTSV.

Materials and methods

Cells

Vero E6 cells (ATCC C1008) were maintained in Eagle's minimum essential medium (EMEM) (Gibco; Thermo Fisher Scientific, MA, USA) supplemented with 5% heat-inactivated fetal bovine serum (FBS) (Biowest, Nuaillé, France), MEM non-essential amino acids (Gibco), insulin-transferrin-selenium (Gibco; Thermo Fisher Scientific), penicillin-streptomycin (50 units/mL, 50 μg/mL; Sigma-Aldrich Co., St Louis, MO, USA), and gentamicin (100 μg/mL; Sigma-Aldrich). Human embryonic kidney (HEK) 293T cells were maintained in Dulbecco's modified Eagle's medium (DMEM; Sigma-Aldrich) supplemented with 10% FBS, penicillin-streptomycin (50 units/mL, 50 μg/mL; Sigma-Aldrich). BHK/T7-9 (RRID: CVCL_A8V7) cells stably expressing the T7 RNA polymerase gene under the control of the beta-actin promoter were kindly provided by Dr. Naoto Ito and Dr. Makoto Sugiyama from Gifu University[23]. The cells were maintained in EMEM supplemented with 5% FBS, 1% penicillin, streptomycin, and 10% tryptone phosphate broth (TPB; Thermo Fisher Scientific). BSR-T7/5 cells stably expressing T7 RNA polymerase were kindly provided by Dr. K. K. Conzelmann (Max-von-Pettenkofer Institut, Munich, Germany)[35]. The cells were maintained in DMEM supplemented with 10% FBS, 10% TPB, and antibiotics (1 mg/mL Geneticin (G418) (Nacalai Tesque, Kyoto, Japan) or penicillin-streptomycin (50 units/mL, 50 μg/mL; Sigma-Aldrich). All cells were cultured in a 5% CO_2 incubator at 37°C.

Virus

The SFTSV YG1 strain was used in this study[5]. Experiments involving viral infections were performed in a biosafety level 3 (BSL-3) facility at the Institute for Genetic Medicine, Hokkaido University. The Vero E6 cells were seeded at 5×10^3 cells/well on 12-well glass slides (Matsunami Glass Ind., Ltd. Osaka, Japan) and incubated at 37°C in a 5% CO_2

incubator for 16 h. The cells were inoculated with virus at a multiplicity of infection (MOI) of 0.1. Twenty hours after inoculation, the slides were fixed with 4% paraformaldehyde phosphate buffer solution (PPBS) (FUJIFILM Wako Pure Chemical Co., Osaka, Japan) for 20 min at room temperature.

Plasmids

The full open reading frames of SFTSV N protein, GP, and RdRp were previously cloned into the pCAGGS-MCS mammalian expression vector as described by Lundu *et al.* and were named pCAGGS-SFTSV N, pCAGGS-SFTSV GP, and pCAGGS-SFTSV L, respectively[22]. A triple mutant gene was synthesized introducing three amino acid mutations (R64/D, K67/D, and K74/D)[24] (GenScript, Tokyo, Japan). The synthesized gene was cloned into the pCAGGS-SFTSV N plasmid and named pCAGGS-SFTSV mt-N. As an alternative to the viral genome, a minus-sense reporter gene, Renilla luciferase (vRNA-Rluc) or eGFP, which mimics the viral genome with untranslated regions of the M segment at both ends using pATX expression vectors named pATX-vRNA-Rluc and pATX-vRNA-eGFP were prepared[25]. Epitope-tagged SFTSV N and mt-N were constructed using primers containing the hemagglutinin (HA) tag sequence as explained elsewhere[22]. The plasmid sequences were confirmed by Sanger sequencing analysis before use.

Expression of recombinant proteins and minigenome

To analyze the subcellular localization of SFTSV structural proteins, the N protein, mt-N protein, GP, RdRp, vRNA-Rluc and T7 polymerase were expressed in various combinations in Vero E6 cells. Briefly, the Vero E6 cells (5×10^3 cells/well) were seeded on 24-well slides (Matsunami) and incubated at 37°C in a 5% CO_2 incubator for 16 h. The cells were transfected using TransIT-LT1 reagent (Mirus Bio LLC, Madison, WI, USA) with a single

expression plasmid or combinations of expression plasmids, including pCAGGS-SFTSV N, pCAGGS-SFTSV mt-N, pCAGGS-SFTSV GP, pCAGGS-SFTSV L, pATX-vRNA-Rluc, pATX-vRNA-eGFP, and pCAGGST7, according to the manufacturer's protocol. After 24 h of incubation, the cells were fixed with 4% PPBS.

Minigenome assay

BHK/T7-9 cells (1×10^5 cells/well) were seeded in a 12-well plate and incubated for 16 h in a 5% CO_2 incubator. The cells were transfected with either pCAGGS-SFTSV N or pCAGGS-SFTSV mt-N together with pCAGGS-SFTSV L, pATX-vRNA-Rluc, and a firefly luciferase expression plasmid for the standardized measurement of gene transfer[25]. The pCAGGS-MCS plasmid without any insertion was used as a negative control. All transfected cells were incubated at 37°C in a 5% CO_2 incubator for 24 h. The culture supernatant of each well was removed, and the cell pellet was lysed using 20 μL of passive lysis buffer (Promega Co., Madison, WI, USA). The cell lysate was reacted with Dual-Luciferase Reporter assay reagents (Promega Co.), and the Renilla luciferase and firefly luciferase activities were measured using the GloMax-Multi Detection System (Promega Co.). Polymerase activity was determined based on the ratio of Renilla luciferase activity to firefly luciferase activity.
All data were presented as mean ± standard deviation. Statistical analysis was performed using a one-tailed Student's t-test. A *P*-value of >0.01 was considered significant.

Indirect immunofluorescence assay

PPBS-fixed cells were permeabilized with 1% Triton X-100 in phosphate buffered saline (PBS) for 10 min and blocked with 1% bovine serum albumin (BSA)/PBS for 30 min. The cells were labeled with rabbit anti-N synthetic peptide (40-54) polyclonal antibody (pAb) (Sigma-Aldrich) or YG1.7-3-3-4 mouse anti-N monoclonal antibody (mAb) (kindly provided

by Prof. Ayato Takada, Hokkaido University), rabbit anti-Gn (#6647) and anti-Gc (#6653) pAb (Prosci Inc., Poway, CA, USA), and rabbit anti-L synthetic peptide (386-400) pAb (Frontier Laboratories, Fukushima, Japan). The organelles were marked with mouse anti-ERGIC-53 (G1/93) mAb IgG1 (Enzo Life Sciences Inc., NY, USA) or rabbit anti- ERGIC53 pAb (Proteintech, IL, USA) and anti-GM130 antibody-cis Golgi marker antibody 169276 (Abcam, Cambridge, UK). Alexa Fluor 488 anti-rabbit IgG, Alexa Fluor 594 anti-rabbit IgG, and Alexa Fluor 594 anti-mouse IgG (Invitrogen; Thermo Fisher Scientific) were used as secondary antibodies. Anti-HA-tag polyclonal antibody labeled with Alexa Fluor 488 (Medical & Biological Laboratories Co., Ltd, Nagoya, Japan) was used to label the HA-tag. The stained cells were mounted with ProLong Gold Antifade reagent with 4′6-diamidino-2-phenylindole (DAPI) (Invitrogen; Thermo Fisher Scientific) according to the manufacturer's instructions. Fluorescent images were acquired using an FV1000-D Olympus confocal microscope (Olympus Co., Tokyo, Japan) with a 100× oil objective lens.

Image analysis

Image analyses of colocalization were performed using the open-source Fiji/ImageJ software[26]. Pearson's correlation coefficient (PCC) and mander's correlation coefficient (MCC) M2 were obtained using the ImageJ plugin "Coloc2."

Immunoprecipitation (IP) assay

BSR-T7/5 cells were transfected with pCAGGS-SFTSV N or pCAGGS-SFTSV mt-N together with pCAGGS-SFTSV-RdRp and pATX-vRNA-eGFP, according to the manufacturer's instructions, and incubated at 37°C in a 5% CO_2 incubator for 24 h. The cells (5×10^5) were rinsed once with ice-cold PBS followed by lysis in 0.5 mL of polysome lysis buffer containing 20 mM Tris-HCl (pH 7.5), 100 mM KCl, 5 mM $MgCl_2$, 0.5% Nonidet P-

40, 100 U/mL RNase inhibitor, and 1× protease inhibitor cocktail. The polysomal lysate was incubated for 20 min on ice to obtain the supernatant after centrifugation. The SFTSV N or SFTSV mt-N protein was immunoprecipitated using Dynabeads Protein A Immunoprecipitation Kit (Thermo Fisher Scientific) according to the manufacturer's protocol. Briefly, the binding antibody used was 5 μg of mouse anti-N mAb or mouse IgG2b, kappa monoclonal [MPC 11] – isotype control (Abcam) – incubated with magnetic beads with rotation for 10 min at room temperature. Subsequently, 250 μL of the polysomal lysate was added to the magnetic bead-Ab complex, followed by several washing steps, and incubated with rotation for 1 h at 4°C. The supernatant was removed from the magnetic beads-Ab-Ag complex after washing, and 1 mL of Isogen (Nippon Gene, Tokyo, Japan) or 20 μL of 2 × SDS sample buffer was added directly into the complex, depending on the following experiment.

Quantitative PCR assay

Total RNA was extracted from the samples acquired from the IP assay according to the manufacturer's protocol and used as a template for reverse-transcription PCR (RT-PCR). RT-PCR was performed using ReverTra Ace qPCR RT Master Mix (Toyobo, Osaka, Japan). The KAPA SYBR FAST for LightCycler 480 Kit (Sigma Aldrich) was used to perform the qPCR reaction using the following primer set: forward primer: 5′-CAAGGAGGACGGCAACATCCTGGG-3′ and reverse primer: 5′-ATGCCGTTCTTCTGCTTGTCGGCC-′3-expressing eGFP gene. qPCR was performed using LightCycler 480 II (Roche Applied Science, Oberbayern, Germany).

Western blotting

HEK293T cells were seeded on a 6-well plate at 3×10^5 cells/well and incubated overnight at 37°C in a 5% CO_2 incubator. The cells were transfected with pCAGGS-SFTSV N, pCAGGS-SFTSV mt-N, or pCAGGS/MCS vector as a negative control and cultured for 24 h. The cells were rinsed once with PBS and lysed by treatment with 4 × Laemmli buffer (Bio-Rad Laboratories, CA, USA) supplemented with 2-mercaptoethanol. The collected cell lysate and samples from the IP assay were incubated at 100°C for 5 min. The prepared samples were subjected to sodium dodecyl sulfate-polyacrylamide gel electrophoresis (SDS-PAGE) using 5%–20% gradient gels (ATTO Co., Tokyo, Japan). After electrophoresis, the proteins were transferred to a 0.45-μm pore immunoblot PVDF membrane (Millipore, Billerica, MA, USA). After blocking the membrane with Block Ace (Dainippon Pharma Co., Osaka, Japan) supplemented with 0.1% BSA for 1–16 hours at 4°C, antibody treatment was performed. A rabbit anti-N polyclonal antibody diluted 1:1000 in Can Get Signal Immunoreaction Enhancer Solution 1 (Toyobo) was used as the primary antibody and was incubated for 1 h at room temperature. Horseradish peroxidase-conjugated protein A (Prozyme Inc., CA, USA) at a 3,000-fold dilution or horseradish peroxidase-conjugated mouse anti-rabbit IgG as the secondary antibody (Jackson ImmunoResearch Laboratories Inc., Baltimore, MD, USA), diluted 10,000 times with Can Get Signal Immunoreaction Enhancer Solution 2 (Toyobo) was used as the secondary antibody and incubated for 1 h at room temperature. After washing with PBS, the proteins were reacted with Amersham ECL Prime (GE Healthcare Life Science, PA, USA) and detected using ImageQuant LAS 4000 mini (GE Healthcare Life Science) according to the manufacturer's protocol.

Results

Localization of N protein in the presence of RdRp and GP in transfected cells

Interaction with GP is an important factor for the localization of viral components into the ERGIC and Golgi apparatus, which is a viral assembly compartment; Lundu *et al.* reported the localization of GP in the presence of N protein. In this study, I reproduced the same results using N protein and GP, especially focusing on the N protein (Figure 1). N protein and GP were co-expressed in Vero E6 cells, and the intracellular localization of N protein was analyzed under a confocal microscope. The N protein was not localized to the ERGIC or Golgi apparatus in the presence of GP, which agrees with the results of previous studies. To further clarify the relationship between GP and RdRp, Icarried out a subcellular localization experiment in which GP and RdRp were co-expressed. RdRp was localized to the ERGIC and Golgi apparatus in the cells expressing GP, which agrees with the results of Lundu *et al*. (Figure 2a)[22]. In Figure 2b*,* I estimated the colocalization using the PCC, which is used to calculate the number of respective coefficients. The PCC value range differs from −1.0 to 1.0, where 0 indicates no significant correlation and 1 indicates a complete positive correlation[27]. The number of cells showing high PCC values in RdRp localization in the presence of GP to the ERGIC was higher than that to the Golgi apparatus. Previous studies reported that the GP of SFTSV is expressed in the ER of infected cells and then moves to the Golgi apparatus via the ERGIC and accumulates in the Golgi apparatus, which suggests that GP plays a major role in leading RdRp to the budding compartments[22]. It is thought that both N protein and RdRp are synthesized in the cytoplasm and then germinate together with GP in the ERGIC to the Golgi apparatus to form viral particles. Next, Vero E6 cells were transfected simultaneously with plasmids of N protein, GP, and RdRp, and the localization of N protein to the ERGIC and Golgi apparatus was examined (Figure 3a). Even in cells simultaneously co-expressing RdRp and GP, the N protein did not localize to the ERGIC or Golgi apparatus.

These results suggest that viral factors other than viral structural proteins are required for viral particle formation. Therefore, to understand the role of vRNA in viral particle formation and interaction of N protein with vRNA and RdRp, I used cells that co-expressed the N protein, RdRp, and vRNA-Rluc (which mimics vRNA), and analyzed the localization of N protein to the ERGIC and Golgi apparatus (Figure 3b). In the presence of RdRp and vRNA-Rluc, N protein was detected in the cytoplasm, but translocation to the ERGIC and Golgi apparatus was not detected.

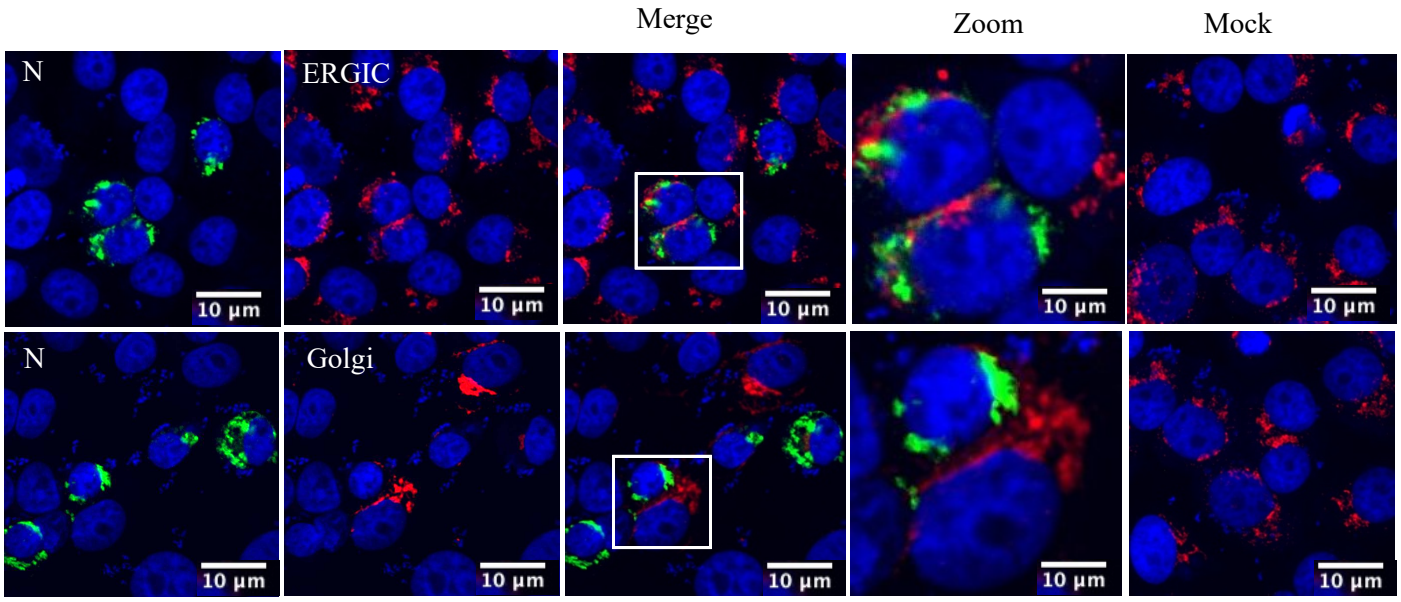

Figure 1. Subcellular localization of N protein in GP transfected cells.

Effect of GP on localization of N protein in Vero E6 cells. Vero E6 cells were transfected with pCAGGS-SFTSV-N and pCAGGS-SFTSV-GP and fixed at 24 hours post-transfection. The cells were stained with antibodies against N protein (Green) and ERGIC (Upper panel) or Golgi organelle markers (Red) (Lower panel), and nuclei were stained with DAPI (Blue). Magnification of the merged area is shown on the right side of the merged image. Mock-transfected cells are shown as mock images.

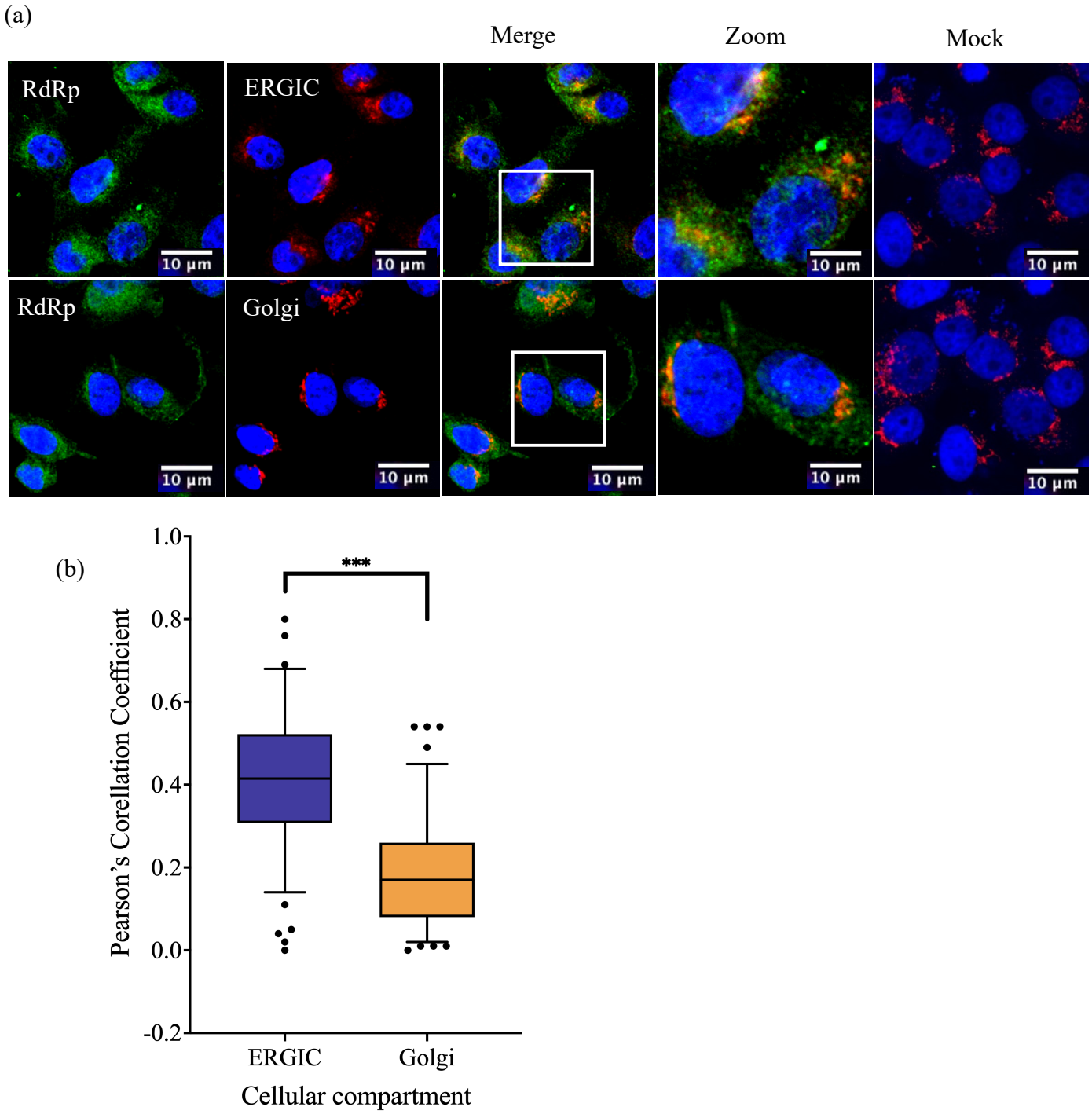

Figure 2. Subcellular localization of RdRp proteins in transfected cells

(a) Cellular localization of RdRp in GP and RdRp co-expressed Vero E6 cells. The cells were stained with antibodies against RdRp (Green) and ERGIC (Upper panel) or Golgi organelle markers (Red) (Lower panel), and nuclei were stained with DAPI (Blue). The yellow areas in the merged image show the colocalization of proteins with the organelle markers. Magnification of the merged area is shown on the right side of the merged image. Mock-transfected cells are shown as mock images.
(b) Co-localization analysis of RdRp and ERGIC or Golgi apparatus by Fiji/ImageJ.

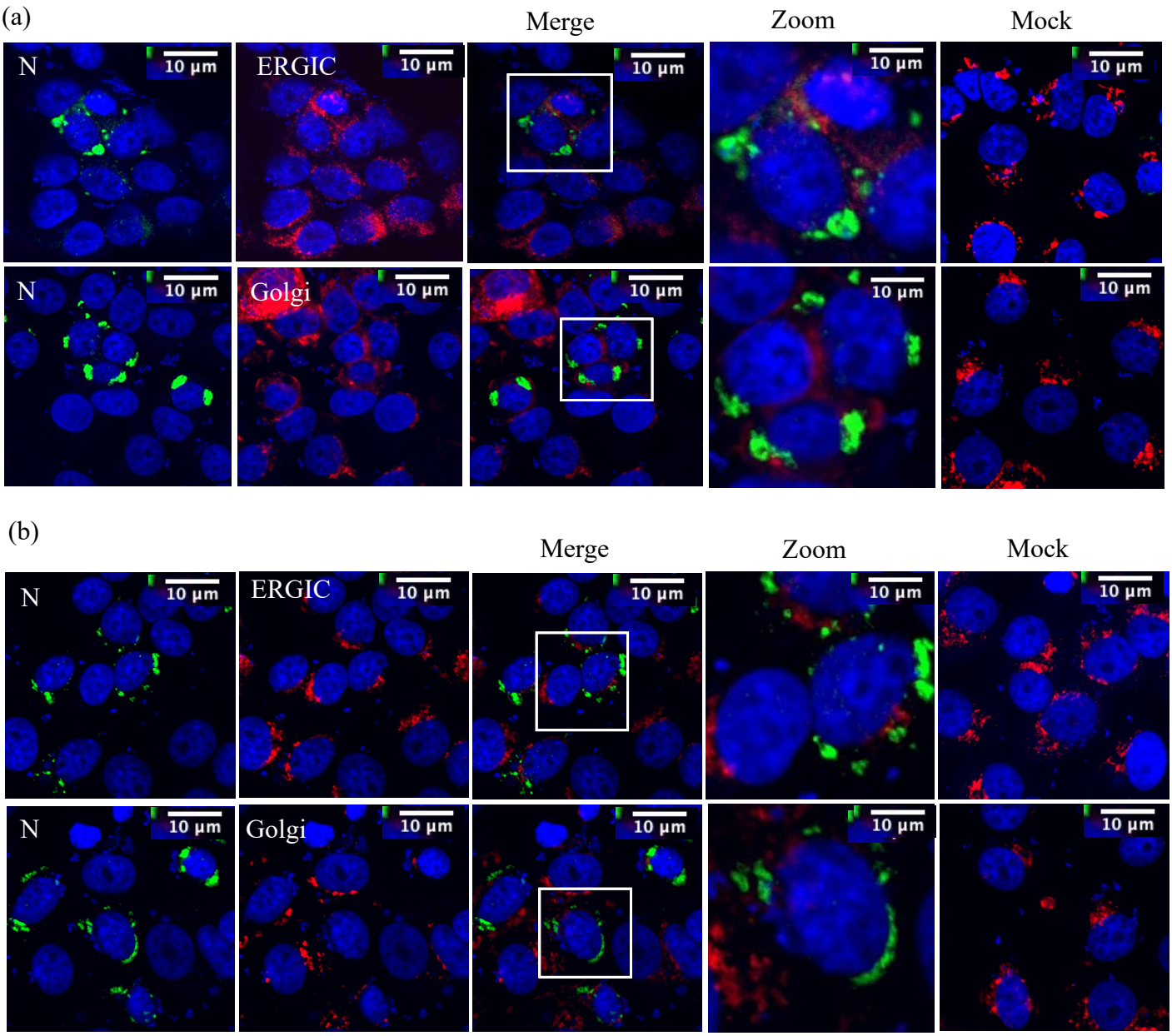

Figure 3. Subcellular localization of N proteins with GP or RdRp

a) Effect of GP and RdRp expression on the localization of N in Vero E6 cells. Vero E6 cells were transfected with pCAGGS-SFTSV-N, pCAGGS-SFTSV-GP, and pCAGGS-SFTSV-RdRp and subsequently fixed at 24 h post-transfection (hpt).
b) Effect of RdRp and vRNA-Rluc on the localization of N in Vero E6 cells. Vero E6 cells were transfected with pCAGGS-SFTSV-N, pCAGGS-SFTSV-RdRp, and vRNA-Rluc and subsequently fixed at 24 hpt. The cells were stained with antibodies against N protein (green) and ERGIC (Upper panel) or Golgi organelle markers (red) (Lower panel), and the nuclei were stained with DAPI (blue). Magnification of the merged area is shown on the right side of the merged image. The mock-transfected cells are shown as mock images. Magnification of the merged area is shown on the right side of the merged image.

Localization of N protein to the ERGIC and Golgi apparatus in cells expressing all viral structural components

Subcellular localization experiments were carried out using all viral structural components, including N protein, GP, RdRp, and vRNA-Rluc. Cellular localization of N protein and GP to the ERGIC and Golgi apparatus in the presence of all viral components was confirmed (Figure 4a). In SFTSV-infected cells N protein, GP, and RdRp colocalized with those of ERGIC and Golgi markers[22]. A significant difference was observed in the PCC value between the presence and absence of GP. Interestingly, the incidence of N protein localization to the ERGIC was higher than that to the Golgi apparatus in the presence of GP (Figure 4b). These results suggest that N protein, GP, RdRp, and vRNA are essential for viral assembly, as was previously shown for hantavirus virion assembly[28].

A minigenome assay was performed by transfecting cells with the N protein, RdRp, and vRNA-Rluc. Luciferase minigenome activity was detected (Figure 4c), indicating that N protein interact with RdRp and vRNA, which mimic the RNP complex in the cell cytoplasm. This finding demonstrates that the expressed N protein functionally interacts with RdRp and vRNA in the cell cytoplasm. However, localization experiments did not confirm the localization of N protein to the ERGIC and Golgi apparatus in cells expressing all viral proteins, except for GP (Figure 3b). Interestingly, a minigenome assay with GP showed decreased luciferase activity compared with that in the minigenome assay of N protein and RdRp, which exhibited the highest luciferase activity (Figure 4c).

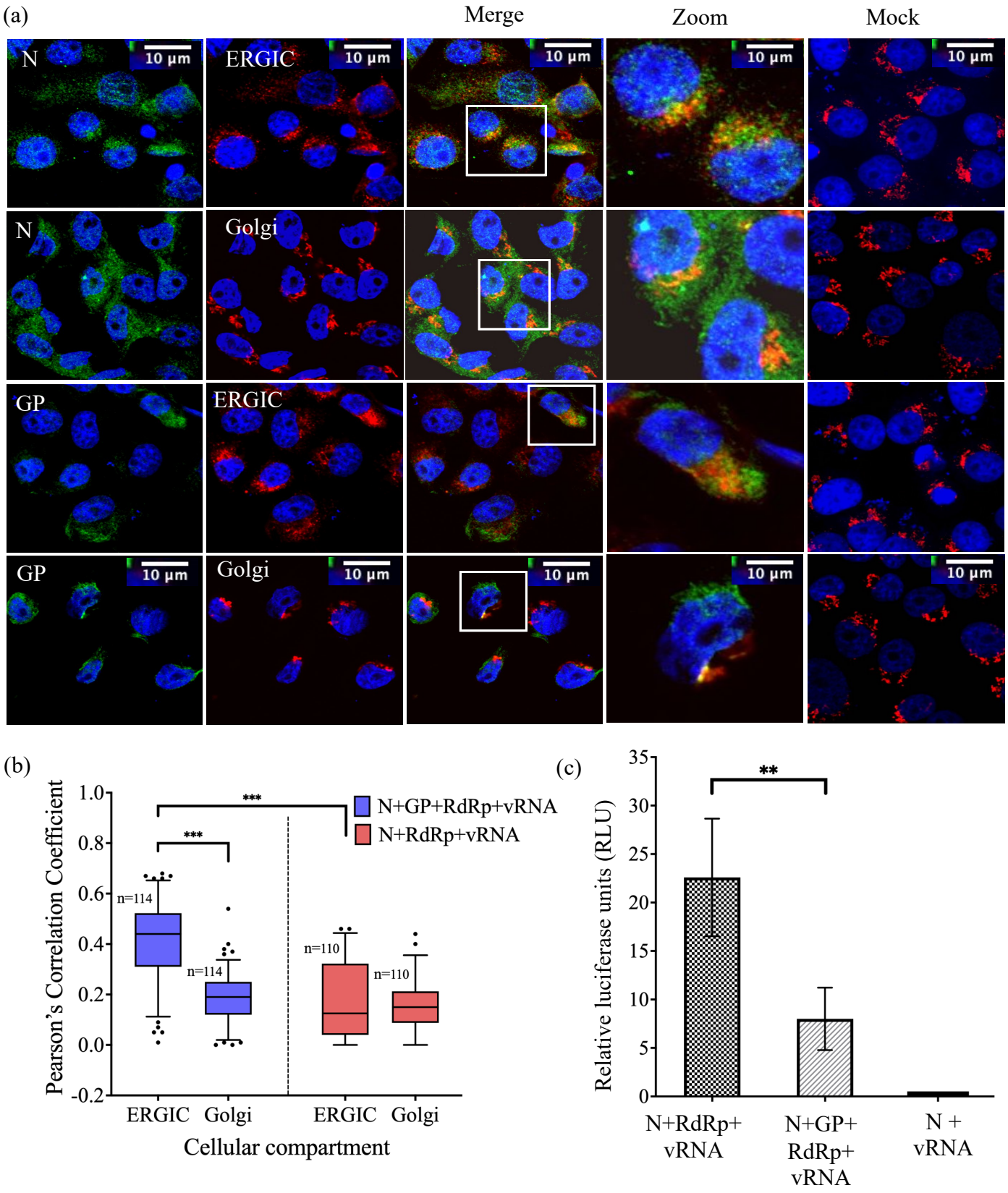

Figure 4. Subcellular localization of N protein together with all viral components

Figure 4. Subcellular localization of N protein together with all viral components

(a) Vero E6 cells were transfected with pCAGGS-SFTSV-N, pCAGGS-SFTSV-GP, pCAGGS-SFTSV-RdRp, and vRNA-Rluc and subsequently fixed at 24 h post-transfection. The cells were stained with antibodies against N protein or GP (green) and ERGIC or Golgi organelle markers (red), and the nuclei were stained with DAPI (blue). The yellow areas in the merged images show the cellular localization of proteins with organelle markers. Magnification of the merged area is shown on the right side of the merged image. The mock-transfected cells are shown as mock images.

(b) The graph showing the colocalization of N with ERGIC, and Golgi apparatus. The images of cells shown in (a) was analyzed using ImageJ and calculated the PCC value of each cell. The quantitative data obtained from image analysis were used to calculate the *P*-value (Corresponding to * $P < 0.05$, ** $P < 0.01$, and *** $P < 0.001$)

(c) Detection of transcriptional activity using a minigenome assay. BHK/T7-9 cells were transfected with pCAGGS-SFTSV-N, pCAGGS-SFTSV-RdRp, and vRNA-Rluc or pCAGGS-SFTSV-N, pCAGGS-SFTSV-RdRp, vRNA-Rluc, and pCAGGS-SFTSV-GP. The luciferase activities were compared with that of N+vRNA-Rluc (without RdRp) as a negative control. The activity of Rluc was standardized by Fluc activity (transfection control). Results are shown as RLUin the bar graph with standard deviations of the means. The statistical significance between RdRp and without RdRp in different combinations was assessed using the Student's t-test (corresponding to *$P < 0.05$ and ** $P < 0.01$).

Interaction of the N protein with vRNA is essential for N protein.

To confirm the importance of the interaction between vRNA and N protein in the localization of the N protein, a plasmid expressing a triple mutant N (mt-N) protein with substitution of three amino acids in the RNA-binding domain was constructed. Three amino acids (R64, K67, and K74) of the RNA-binding site were substituted with amino acid D, and pCAGGS-SFTSV mt-N was prepared[24]. The expression of mt-N protein was confirmed by western blotting (Figure 5a). In a minigenome assay, the luciferase activity of mt-N protein was almost the same as that of the negative control, suggesting that the conformation of a functional RNP complex was inhibited by the mutation in the N protein (Figure 6).

An IP assay using an SFTSV anti-N antibody was conducted to investigate the interaction between N and minigenome RNA. First, the enhanced green fluorescent protein (eGFP) expression was confirmed by transfecting pATX-vRNA-eGFP into BSR-T7/5 cells (Figure 5b). Following the IP assay, the presence of both N and mt-N proteins was confirmed by western blotting (Figure 5c). Quantitative polymerase chain reaction PCR (qPCR) was performed by targeting the eGFP gene to identify if the N protein co-immunoprecipitated with minigenome RNA. The RNA copy number of the N protein was higher than that of the mt-N protein in the qPCR assay, which indicates the lack of mt-N binding to RNA (Figure 5d).

The localization of mt-N protein in cells co-expressing RdRp, GP, and vRNA-Rluc was analyzed. The mt-N protein did not localize to the ERGIC and Golgi apparatus, in contrast to the N protein (Figure 5e and 4a). HA-tagged N protein and mt-N protein were transfected into the SFTSV-infected BHK/T7-9 cells to understand the organization of N protein in infected cells. HA-tagged N protein was localized to the ERGIC and Golgi apparatus, whereas mt-N did not localize to these areas (Figure 5f). The Mander's correlation coefficient (MCC) M2 was used to evaluate the colocalization of green pixels to red pixels between the

HA-N or HA-mt N protein to the ERGIC and Golgi apparatus (Figure 5g). Its values are in the range from -1.0 to 1.0.[27]. The HA-N protein showed a significant correlation with the ERGIC, and Golgi apparatus compared with the mt-N protein. Interestingly, the incidence of N protein localization to the ERGIC was higher than that to the Golgi apparatus in both N and mt-N proteins which agrees with the results of Figure 4. These results show that the interaction between the N protein and viral RNA is indispensable for the localization to the ERGIC and Golgi apparatus.

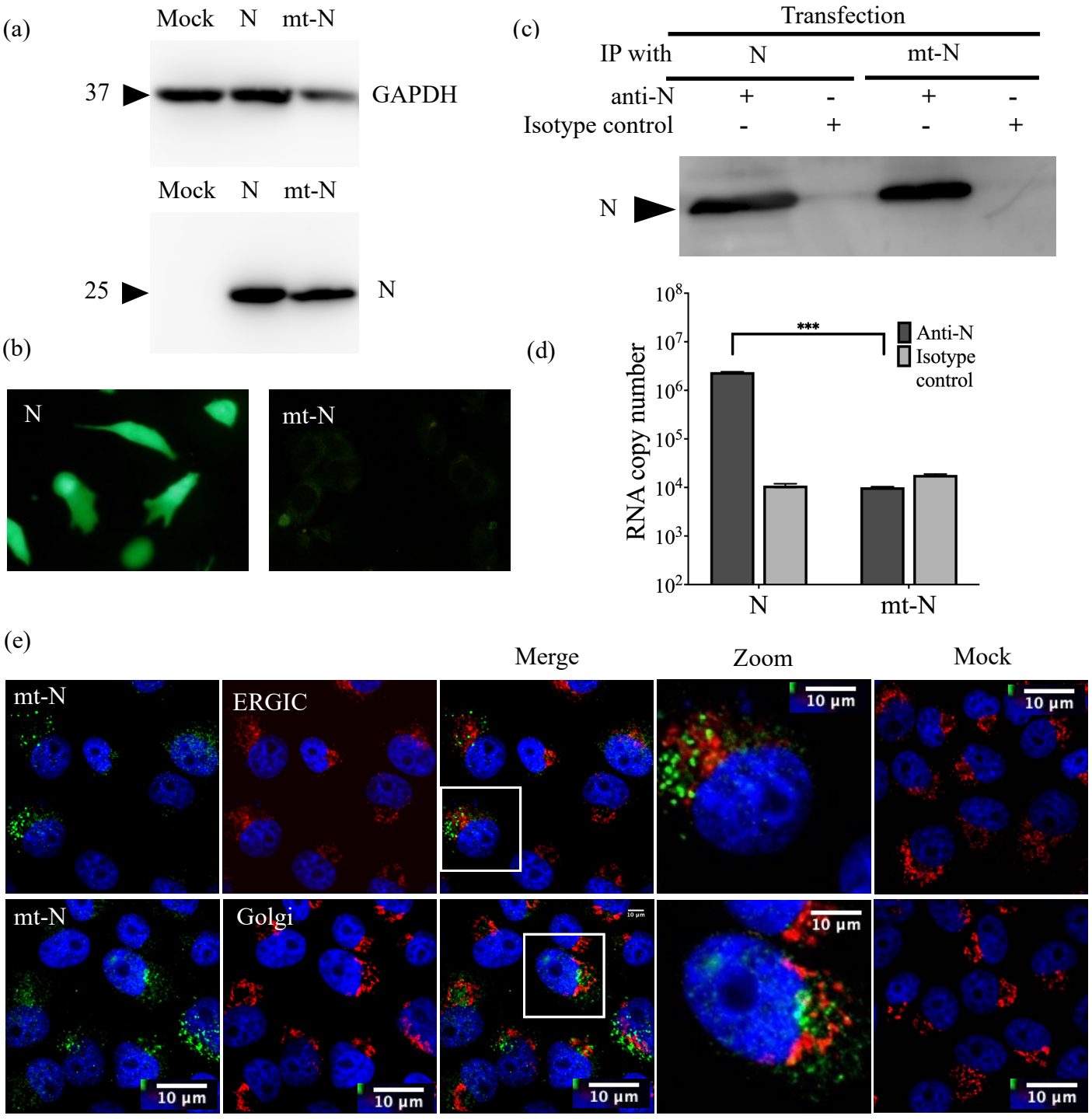

Figure 5. Localization analysis of N and mt-N proteins of SFTSV

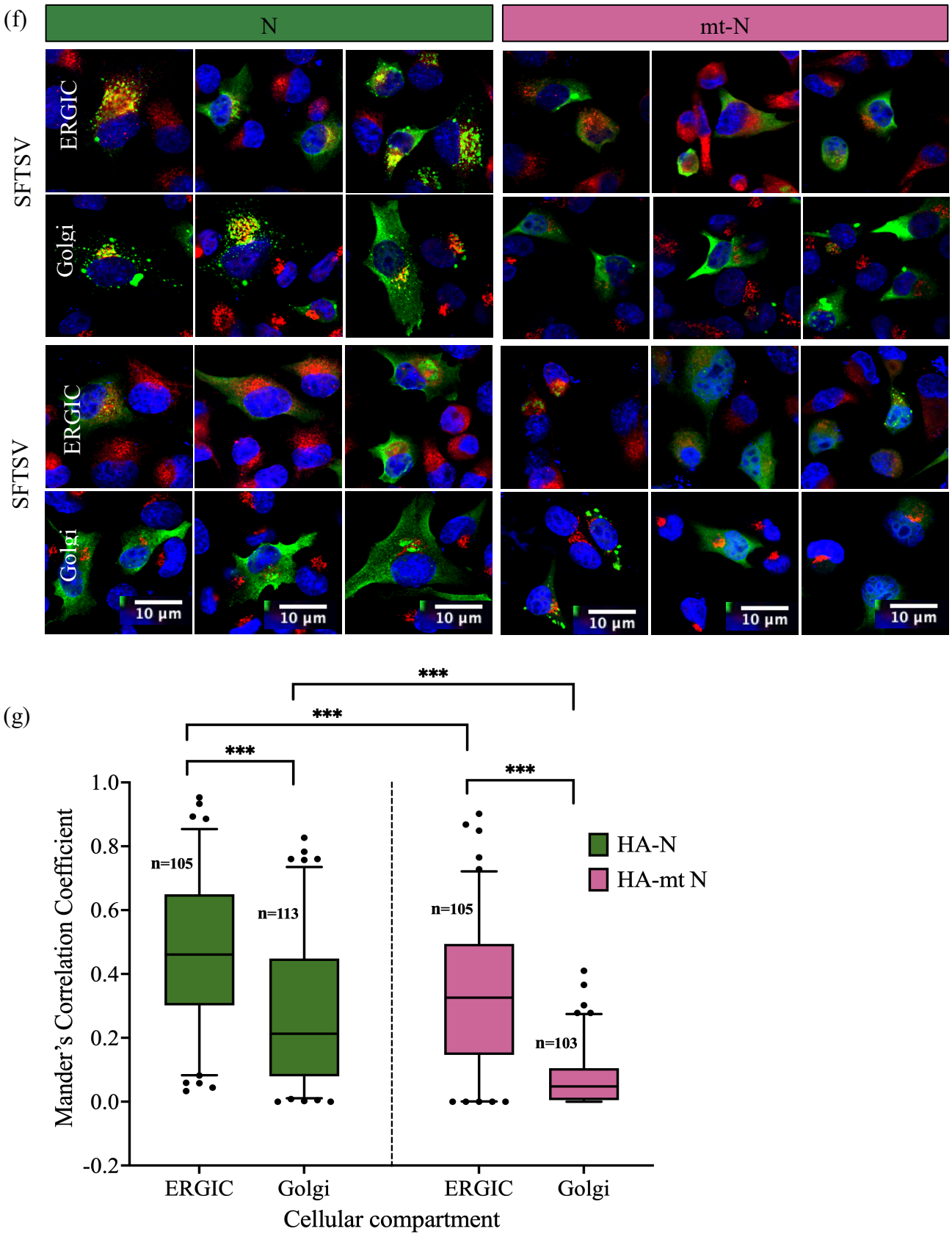

Figure 5. Localization analysis of N and mt-N proteins of SFTSV

Figure 5. Localization analysis of N and mt-N proteins of SFTSV

(a) The cell lysate of mt-N protein-transfected 293T cells was used for western blot analysis, and expressed proteins were determined using anti-rabbit N polyclonal antibody as the primary antibody and HRP-conjugated Protein A as the secondary antibody. GAPDH was used as a control.
(b) BSR-T7/5 cells were transfected with pCAGGS-SFTSV N or pCAGGS-SFTSV mt-N together with pCAGGS-SFTSV-RdRp and pATX-vRNA-eGFP and eGFP expression was examined.
(c) Cell lysates from (b) were immunoprecipitated with anti-N. Both N and mt-N proteins successfully bound to the beads and were detected by western blotting using rabbit anti-N pAb.
(d) Minigenome RNA was detected from immunoprecipitated fraction by qPCR of eGFP gene. (Corresponding to * $P < 0.05$, ** $P < 0.01$, and *** $P < 0.001$)
(e) Subcellular localization of the mt-N protein in Vero cells. Plasmids pCAGGS-SFTSV-mt-N, pCAGGS-SFTSV-RdRp, pCAGGS-SFTSV-GP, and vRNA-Rluc were transfected, and the luciferase activity was not detected in these cells. The cells were stained with antibodies against N protein (green) and ERGIC or Golgi organelle markers (red), and the nuclei were stained with DAPI (blue). Magnification of the merged area is shown on the right side of the merged image. The mock-transfected cells are shown as mock images.
(f) Sub-cellular localization of HA-tagged N and HA-tagged mt-N proteins in SFTSV-infected BHK/T7-9 cells. SFTSV-infected BHK/T7-9 cells were transfected with pCAGGS-SFTSV-N or pCAGGS-SFTSV mt-N. The cells were stained with antibodies against HA-tag protein (green) and ERGIC or Golgi organelle markers (red), and the nuclei were stained with DAPI (blue). The mock-infected and transfected cells are shown as SFTSV (−).
(g) Co-localization analysis of HA-tagged N and mt-N proteins with Golgi apparatus markers shown in (f) using Fiji/ImageJ (***corresponds to a P value of <0.001).

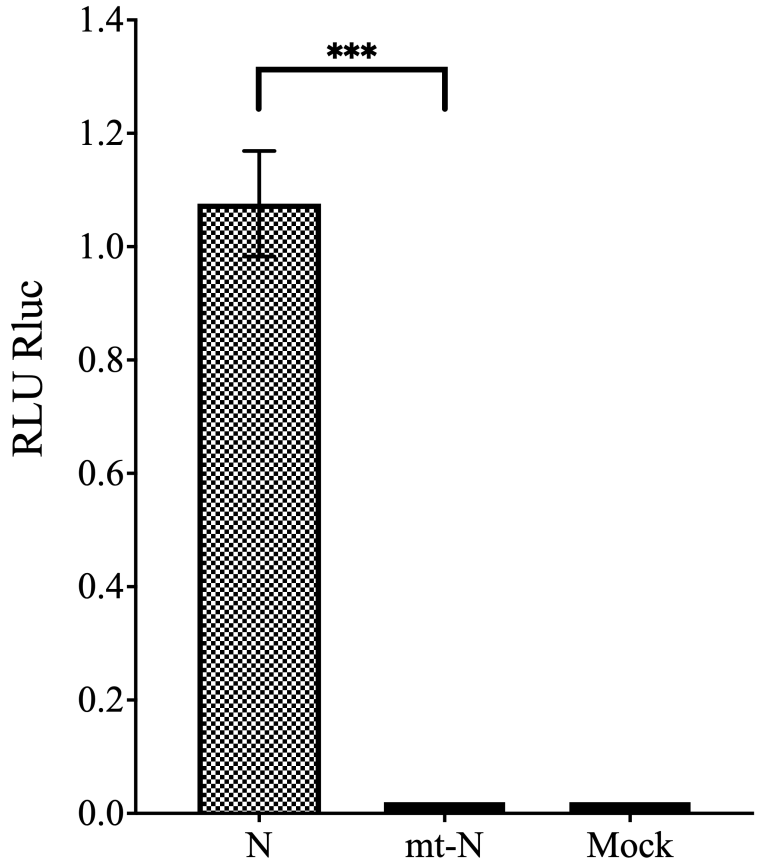

Figure 6. Functionality of mt-N protein of SFTSV.

Detection of transcriptional activity by a minigenome assay. N protein or mt-N protein was transfected into BHK/T7-9 cells together with RdRp and vRNA-Rluc, and the luciferase activities were compared. Mock-transfected cells are shown as mock images. (**corresponds to a P-value < 0.01.)

Discussion

Most of the negative-strand RNA viruses require a host cell secretory pathway for viral infection; the transportation of cellular proteins and cargo from the Golgi apparatus to the ER via the ERGIC has been reported[18,29]. Most of the viruses belonging to the order *Bunyavirales* use not only the ER and Golgi apparatus, but also the ERGIC as site of virion assembly[21,30,31]. The locations of viral structural proteins are indispensable for infectious viral particle formation[18,28,30,32-34]. Previous studies showed that RdRp was partially localized to the ERGIC and Golgi apparatus in the presence of GP, whereas N protein was widely expressed in the cytoplasm, even in cells coexpressing GP[22]. In this study, I showed that the interaction between the N protein and viral RNA plays a critical role in the intracellular transportation of N protein to the ERGIC and Golgi apparatus. Thus, N protein translated into the cytoplasm forms an RNP complex together with vRNA to further interact with GP localized in the ERGIC via RdRp to be taken up by virus particles.

In bunyavirus particle formation, the N protein is essential for the transcription and replication of vRNA along with RdRp[35].Multiple copies of the N protein coat each segment of vRNA and forms a functional RNP complex together with the L protein of one RdRp. The N protein coating of the vRNA is thought to play a role in protecting vRNA from the host defense mechanisms. The RNP complex interacts with GP in RNP packaging to be incorporated into particles in the Golgi apparatus where GP is accumulated[36-38]. The GP of the Uukuniemi virus which belongs to the order *Bunyavirales* and family *Phenuiviridae* is translated by ribosomes on the ER and that viral particle formation occurs in the ERGIC and budding continues in the Golgi apparatus[21]. Moreover, ERGIC is an important organelle for intracellular transport and particle formation of bunyaviruses and that N proteins are transported by the action of microtubules[21,28]. Lundu *et al.* reported that viral structural proteins in SFTSV-infected cells were localized in the ERGIC and Golgi apparatus, which are

important cell components for virion formation[22]. Furthermore, the Gn of RVFV is localized in the Golgi apparatus alone, whereas RdRp is localized together with Gn in the Golgi apparatus[33]. Similarly, in SFTSV, only GP was localized in the ER, ERGIC, and Golgi apparatus, but RdRp was partially localized in the ERGIC and Golgi apparatus in the presence of GP. By contrast, N protein was not localized in the ERGIC and Golgi apparatus, even in the presence of GP[22]. These findings suggest that N protein is not directly bound to GP or RdRp, but is necessary for translocation to the ERGIC or Golgi apparatus for virion formation.

In the present study, the viral genome was simultaneously expressed with viral structural proteins. vRNA-Rluc or vRNA-eGFP was used as an alternative to vRNA to conduct experiments safely at the BSL2 facility. As a result, it was confirmed that the N protein, RdRp, GP, and RNA mimicking vRNA, when simultaneously introduced into the cells, resulted in the localization of the N protein in the ERGIC and Golgi apparatus. These results suggest that localization of the N protein in the ERGIC and Golgi apparatus requires association with RdRp and vRNA. The results of our study are consistent with a previous studies showing that N protein forms a multimer in the RNP complex and wrapping around the vRNA, and with the RdRp interactions with the vRNA which occurs by direct contacts with the 5′ and 3′ ends of the vRNA[39,40]. On the contrary, in any other combination of viral structural proteins with the viral genome, the N protein could not be fully localized to the ERGIC nor to the Golgi apparatus.

In the confocal microscopy images, localization of the N protein in the presence of vRNA-Rluc was not detected in the ERGIC and Golgi apparatus. In contrast, luciferase minigenome activity was detected, and the level of activity was higher than the level of luciferase activity with GP (Figure 4c). This finding indicated that even though the RNP complex functions as a transcription complex in the cell cytoplasm when it interacts with GP in RNP packaging in

the ERGIC or Golgi apparatus. Further, in the cellular compartments where occur transcription does not occur packaging. This mechanism might be affected by other cellular factors, which requires further investigation.

Mutations involved in the binding of SFTSV N protein to vRNA have been identified (R64/D, K67/D, K74/D)[24]. In this study, I used an mt-N protein with the substitution of three amino acids that are important for the binding of N protein to vRNA. In addition, Jiao *et al*. did not verify the lack of mt-N binding to RNA. Therefore, an IP assay using an anti-N antibody was conducted to investigate the binding between the N protein and the minigenome RNA. As a result, Iwere able to provide evidence of the mt-N protein's lack of ability to bind to RNA. Due to the same reason, the mt-N protein could not be sorted to the ERGIC and Golgi apparatus even in the presence of RdRp, GP, and vRNA. This finding suggests that the interaction between the N protein of SFTSV and vRNA is important for the localization of viral proteins. On the contrary, unexpected structural defects in the N protein caused by mutations other than the lack of RNA-binding ability could inhibit RNP assembly. A proper interaction of the N protein with vRNA and RdRp is required for the transcription of the RNP complex and for localization of structural proteins to the ERGIC and Golgi apparatus.

To distinguish between the orderly process of natural infection and overexpression phenomenon in transfection experiments, Iconducted experiments using HA-tagged N and mt-N proteins. This led us to understand the sorting of N proteins in infected cells. HA-tagged N protein was localized to the ERGIC and Golgi apparatus, whereas the mt-N protein did not localize to these areas. In the overexpressed systems shown in this study, abundant accumulation was observed in the ERGIC but not in the Golgi apparatus. Also, the similar pattern was observed in the natural infection. Further studies needed to determine the distribution of N proteins in all cellular compartments. Further investigations are needed to

understand the differences and/or similarities between the overexpression system and process of natural infection.

In some enveloped viruses, such as murine leukemia virus and Ebola virus, an interaction between the viral RNP complex and envelope proteins facilitates the budding of virus particles[41,42]. In some other enveloped viruses such as coronavirus and Marburg virus, RNPs play a critical role in the viral envelope formation and virus particle production[43,44].

In the IP assay, I attempted to demonstrate the binding of RdRp using Western blotting; however, I could not obtain a proper image that could withstand publication. Thus, the results of this study do not convincingly show the formation of an RNP complex or the exact interaction between GP and the RNP complex. The cytoplasmic tails of GP of Uukuniemi virus can directly interact with N protein to enable the packaging of RNPs into virus particles[45]. Therefore, further studies are needed to understand the interaction between Gn/Gc and the N proteins of SFTSV.

Overall, the findings of this study will shed light on the basic process of the SFTSV life cycle. This will be useful for developing specific inhibitors interfering with N protein and vRNA and antiviral strategies against SFTSV.

In conclusion, I focused solely on the nuclear protein N protein and analyzed the interaction between vRNA, and other viral proteins required for intracellular localization of N protein. Further studies are needed to clarify the details of intracellular pathways such as N protein or RdRp synthesis and RNP complex formation that occurs in the cytoplasm. Such studies will lead to a full understanding of the SFTSV life cycle and virus particle formation.

Brief Summary

SFTSV is an emerging bunyavirus that causes novel zoonotic diseases in Asian countries including China, Japan, South Korea, and Vietnam. In phleboviruses, viral proteins play a critical role in viral particle formation inside the host cells. Viral GP and RdRp are colocalized in the Golgi apparatus and ERGIC. The N protein was widely expressed in the cytoplasm, even in cells coexpressing GP. However, the role of SFTSV N protein remains unclear. In this study I used different approaches to understand the interaction of N protein, L protein and vRNA and their roles in the RNP complex formation. I constructed a minus-sense reporter gene-eGFP with untranslated regions of the SFTSV M segment at both ends using T7 promoter-expression vector for minigenome-system as a functional alternative to viral genome to use in the immunoprecipitation assay. Sub-cellular localization studies were done by using minigenome assay and confocal microscopy followed by the indirect immunoprecipitation assay. The N protein interacts with vRNA and further shows translational activity with RdRp which is L protein and localized in the ERGIC and Golgi apparatus when co-expressed with GP. On the other hand, mutant N protein did not interact with vRNA either localized in the ERGIC or Golgi apparatus. Interestingly, a minigenome assay with GP showed decreased luciferase activity compared with that in the minigenome assay of N protein and L protein, which exhibited the highest luciferase activity. These results suggest that there is a necessity for functional RNP complex formation with vRNA for localization of N protein to the ERGIC and Golgi complex and, viral assembly. The findings of this study provides useful insights into the life cycle of SFTSV, which will lead to the detection of antiviral targets.

Chapter 2

Characterization of SFTSV Japanese isolate, YG1 strain quasi-species using reverse genetics approaches.

Introduction

SFTS is caused by the SFTSV, a member of the order *Bunyavirales* and the family *Phenuiviridae*. The SFTS is widely distributed in East Asian countries, including China, Japan, South Korea, and Vietnam. The mortality rate of SFTS reaches up to 30% in Japan. The SFTSV YG1 strain was isolated from the first SFTSV patient in Yamaguchi prefecture in Japan[5].

SFTSV S segment is an ambi-sense RNA encoding N and NSs proteins[46], the M segment encodes two envelope GPs; Gn and Gc, whereas; the L segment encodes RdRp.

The viruses of family *Phenuiviridae*, virus entry into host cells initiated by the binding of the GP (Gn and Gc) to cell surface receptors and endocytosis occurred in receptor mediated manner[47]. Followed by the endocytosis, the fusion of viral GP with the endosomal membrane takes place under acidic conditions causing low-pH-dependent cell fusion in infected cells[7,8]. Some amino acid residues of SFTSV Gn and Gc are crucial for low pH-dependent cell fusion and syncytium formation[11,48]. However, the specific function of SFTSV Gn and Gc in cell fusion is yet to be described.

Followed by the cell entry, the infected cells of the viruses in *Phenuiviridae* such as SFTSV and the RVFV can cause a cytopathic effect (CPE)[9,10]. Gao et al reported that the cell death induced in human microglial HMC3 cells by infection of SFTSV was performed by the NOD-like receptor protein 3 (NLRP3) inflammasome activation and leading secretion of interleukin (IL)-1β and pyroptosis[49]. On the other hand, most line and primary culture cells were not killed by SFTSV infection. Suzuki et al reported that B cells were target cells in lethal infection of SFTSV[50]. However, transformed B cells and primary culture of peripheral B cells did not die with SFTSV infection. Vero E6 cells and Huh7 cells used for virus isolation also do not show CPE. The relationship between SFTSV infection and cell death remains largely unknown.

In a previous study, our research team has established three subclones termed E3, A4, and B7 from YG1 strain using the limiting dilution method with the pH-dependent cell fusion activity and CPE. Subclone E3 has a genome identical to the parental YG1 strain, whereas subclones A4 and B7 have two amino acid mutations in glycoproteins: Gn (Y328H) and Gc (R624W). Subclone B7 has another amino acid mutation, N1891K, in RdRp[9]. Subclone A4 (Gn :Y328H, Gc:R624W) showed intense cell fusion activity under acidic conditions. In contrast, B7 (Gn :Y328H, Gc:R624W, RdRp:N1891K) showed robust CPE, indicating the involvement of RdRp N1891K in the difference in CPE of subclones[9]. Also, the polarization of the amino acid at position 1891 of the L protein is critical for its function especially with polymerase activity[25]. The Gn:Y328H mutation was found in 25% of the virus population in patient blood in next-generation sequencing[51](Table 1). On the other hand, two mutations, R624W in Gc and N1891K in RdRp, seemed infrequent. However, the roles of these mutations on the virological characteristics and population structure of SFTSV were not clarified yet. Predicting the emergence and survival of viruses whose pathogenicity changes one mutation to another, is considered important for understanding the pathogenicity of viruses.

In this study, I developed recombinant viruses bearing single mutations using the reverse genetics system to compare the unique virological characteristics carried by each mutation[52]. Then, the selection and survival of viruses containing mutations related to cell fusion and cell death will be assessed and discussed to understand the pathogenicity of YG1 quasispecies.

Table 1. Frequency of variation analyzed in this study estimated by Next Generation Sequencing data of the patient blood in Japan.

Viral protein: Amino acid	**Percentage of population in patient serum sample**	**Percentage of population after virus isolation by Vero E6 cells**
Gn 328: H	26.9%	Around 10%
Gc 624: W	Under-detection	Under-detection
RdRp 1891: K	Under-detection	Under-detection

Yoshikawa *et al.,* 2015 (Values were supplied from authors' personal communication)

Materials & Methods

Cells and Viruses

Vero E6 cells (ATCC C1008) were maintained in EMEM (Thermo Fisher Scientific) supplemented with 5% heat-inactivated FBS (Biowest), 1% MEM non-essential amino acids (Gibco), 1% insulin-transferrin-selenium (Thermo Fisher Scientific), penicillin-streptomycin (50 units/mL, 50 μg/mL; Sigma-Aldrich), and gentamicin (100 μg/mL; Sigma-Aldrich). BSR-T7/5 cells stably expressing T7 RNA polymerase were kindly provided by Dr. K. K. Conzelmann (Max-von-Pettenkofer Institut, Munich, Germany)[53]. The cells were maintained in DMEM-low glucose (Sigma-Aldrich) supplemented with 10% FBS, 10% Tryptose phosphate broth (TPB; Gibco), and antibiotics (1 mg/mL Geneticin (G418) (Nacalai Tesque, Kyoto, Japan) or or penicillin-streptomycin (50 units/mL, 50 μg/mL; Sigma-Aldrich). Huh7 human hepatoma cells and HEK293T cells (Riken, Japan) were grown and maintained in DMEM (Thermo Fisher Scientific) supplemented with 10% FBS and penicillin-streptomycin (50 units/mL, 50 μg/mL; Sigma-Aldrich). All cells were cultured in a 5% CO_2 incubator at 37 °C. Subclones of YG1 strain, A4, E3, and B7, were used as the controls of the experiments. Experiments involving viral infections were performed in BSL-3 facility at the Institute for Genetic Medicine, Hokkaido University according to the National University Corporation Hokkaido University Biosafety Management Regulations on Pathogens and Other Hazardous Agents.

Plasmids

The full-length YG1 S, M, and L segment constructs were generated by cloning into TVT7R (0,0) kindly provided by Dr. Benjamin Brennan, Glasgow center for virus research, Scotland, United Kingdom (Addgene plasmid # 98631 ; http://n2t.net/addgene:98631 ;

RRID:Addgene_98631)[54]. Cloning was carried out using an In-Fusion HD cloning kit (Takara Bio, CA, USA) and was named pTVT7_YG1_S, pTVT7_YG1_M, pTVT7_YG1_L. The amino acid mutation; Y328H was introduced to the pTVT7_YG1_M construct using site-directed mutagenesis using KOD One PCR Master Mix (Toyobo) and primers containing the mutation (Forward: CGTGTCAGACCAAAATGCCATGGTTTCTCCAGAATGA, Reverse: TCATTCTGGAGAAACCATGGCATTTTGGTCTGACACG). The mutation N1891K was introduced to the pTVT7_YG1_L construct, and R624W was introduced to pTVT7_YG1_M using In-Fusion HD cloning kit (Takara Bio), primers containing mutation for insert sequence (Forward: AACTTGGAAGTGCTTTGTGGTAGG), Reverse: GACCAGGCCCAATTGTCAAGAGTTTTC and primers containing mutation for vector sequence (Forward: CAATTGGGCCTGGTCACATGCCTCAGTTC, Reverse: AAGCACTTCCAAGTTCATCTGGGCGTCT). The CAG_YGI_L and CAG_YG1_N1891K were constructed introducing the full open reading frames of SFTSV L and L(N1891K) proteins to the mammalian expression vector pCAGGS-MCS vector. In-fusion cloning kit was used with overlapping primers of CAG_YG1_L insert (Forward: GGTAGGATAAACGTGGAGAATGGG, Reverse: GACCAGGCCCAATTGTCAAGAGTTTTC) and primers of CAG_YG1_L vector (Forward: CAATTGGGCCTGGTCACATGCCTCAGTTC, Reverse: CACGTTTATCCTACCACAAAGCACTTCC). CAG_YG1_N1891K also used the In-Fusion cloning using primers for insert sequence (Forward: GGTAGGATAAACGTGGAGAATGGG, Reverse: GACCAGGCCCATTTGTCAAGAGTTTTC) and primers for vector sequence (Forward: CAAATGGGCCTGGTCACATGCCTCAGTTC, Reverse: CACGTTTATCCTACCACAAAGCACTTCC). All experiments using genetically modified

organisms were conducted in accordance with Hokkaido University Safety Management Regulations on Genetic Recombination Experiments.

Pseudotype virus assay

The mammalian expression vector pCAGGS-YG1 GP and mutants were cloned previously[11]. The pseudotype vesicular stomatitis virus (VSV) possessing GFP and luciferase genes instead of glycoprotein gene was kindly provided by Dr. Heinz Feldmann, DIS, NIAID, NIH. To generate the pseudotyped VSV enveloped with SFTSV GP and mutant GP (VSVdG-SFTSVGP), 293T cells were transfected with each plasmid vector pCAG-GP-Y/R, pCAG-GP-H/R, pCAG-GP-Y/W, pCAG-GP-H/W, using TransIT-LT1(Mirus Bio LLC, Madison, WI, USA) and incubated at 37°C for 30 h. Pseudotype VSV possessing VSV-G were inoculated and each culture supernatant was collected at 13 h after inoculation. Produced VSV particles in the collected supernatants were evaluated by Western blot assay using anti-VSV M monoclonal antibody (kindly provided by Prof. Ayato Takada, Hokkaido University). Vero E6 cells were inoculated with 10-times dilution of each of VSVdG/SFTSV (GP-Y/R, GP-H/R, GP-Y/W or GP-H/W) and incubated at 37°C for 18 h. Luciferase activity in the cell lysate was determined by steady-Glo luciferase reagent (Promega Co.). The degree of the cell entry is directly proportional to the Renilla Luciferase units (RLU) that normalized with Firefly luciferase activity.

Recombinant virus generation

Eight different recombinant viruses were generated by transfecting 4 x10^5 cells/mL BSR-T7/5 cells with 2μg of each pTVT-based plasmids expressing viral genomic segments with or w/o point mutations (Table 1), 0.2μg pTM1-HB29ppL, 1μg pTM1-HB29N kindly provided by Dr. Benjamin Brennan, Glasgow center for virus research, Scotland, United Kingdom

(Brennan et al., 2015). Transfection experiments were carried out using a TransIT-LT1 reagent, and after five days of incubation, the supernatant containing recombinant viruses was harvested as passage 1(P1). Then, the P1 supernatant was blindly passed into the Vero E6 cells, and recombinant virus stock was prepared by harvesting the culture medium at 7-9 days post-infection (dpi), depending on the CPE.

The recombinant virus stock was inoculated into Vero E6 cells for the virus amplification and seed virus was obtained following the 6 days of incubation. The eight rescued viruses were named after their mutations for easy application (Table 2). Total RNA was extracted from the cells using ISOGEN (Nippon Gene, Tokyo, Japan) and the culture supernatant using ISOGEN-LS (Nippon Gene) according to the manufacturer's protocol. The qPCR was performed using ReverTra Ace qPCR RT Master Mix (Toyobo). The KAPA SYBR FAST for LightCycler 480 Kit (Sigma-Aldrich) was used to perform the qPCR reaction using the following primer set: forward primer: 5′- AGCAGCGTCTCACCAAATCTC -3′ and reverse primer: 5′- GCAGGAGCTGAGCGCACTGT -′3- by targeting the SFTSV-YG1-L segment. qPCR was performed using LightCycler 480 II (Roche).

Their nucleotide sequences of rescue viruses were determined using the native barcoding genomic DNA protocol of MinION Sequencing (Oxford Nanopore Technologies, Oxford, UK) and Sanger Sequencing to confirm that no mutation had occurred during the rescue. Recombinant virus rescue experiments were conducted after confirmation by the Minister of Education, Culture, Sports, Science and Technology, Japan.

Table 2. Recombinant viruses and the respective plasmid constructs used for the reverse genetics system.

Recombinant viruses	S genome	M genome 328/624 (Gn/Gc)				L genome 1891	
	-	Y/R	H/R	Y/W	H/W	N	K
rGn	+	-	+	-	-	+	-
rGc	+	-	-	+	-	+	-
rL	+	+	-	-	-	-	+
rGn/L	+	-	+	-	-	-	+
rGc/L	+	-	-	+	-	-	+
rGn/Gc	+	-	-	-	+	+	-
rGn/Gc/L	+	-	-	-	+	-	+
rYG1	+	+	-	-	-	+	-

Indirect immunofluorescence assay (IFA)

PPBS- fixed transfected Vero E6 cells were permeabilized with 1% Triton X-100 in PBS for 10 min and blocked with 1% BSA/PBS for 30 min. The cells were labeled with rabbit anti-L synthetic peptide (386-400) polyclonal antibody (Frontier Laboratories, Fukushima, Japan) and Alexa Flour 488 anti-rabbit antibody (Thermo Fisher Scientific) was used as the secondary antibody. The cells were mounted with ProLong Gold antifade reagent (Invitrogen; Thermo Fisher Scientific) followed by the DAPI staining (Invitrogen) according to the manufacturer's instructions. Fluorescent images were obtained using FV1000-D confocal microscopy (Olympus Co., Tokyo, Japan).

Acetone-fixed infected Vero E6 cells with recombinant viruses were stained with Alexa Fluor 488 conjugated SFTSV YG1.7-3-3-4 mouse anti-N monoclonal antibody (mAb) (kindly provided by Prof. Ayato Takada, Hokkaido University). Fluorescent images were acquired using a fluorescence microscope on 2 dpi.

Virus titration by plaque assay

Vero E6 cells were seeded at 4 x10^5 cells/mL in a 6-well plate, infected with serial dilutions of each recombinant virus, and cultured under an overlay medium: MEM containing 0.8% SeaKem ME agarose (Takara) and 4%FBS. After 7 dpi, 2 mL of neutral red solution (0.1mg/mL in MEM; Sigma-Aldrich) was added to the overlay medium. After incubation of 24 h, viral foci were visible, and the virus titer of each recombinant virus was calculated (Virus titration = Number of viral foci x virus dilution titer). Plaque forming units (PFU) were calculated using the virus titer.

Cell fusion assay

Vero E6 cells were infected with serial dilutions of each recombinant virus and incubated for 7 days at 37°C. The medium was replaced with 50 mM acetate-buffered saline with pH 5.6 and incubated for 2 min at room temperature. Then the acetate buffer was replaced with a fresh growth medium and incubated for 24 hours at 37°C. The cells were fixed with Mildform 10NM; 10% Formalin neutral buffer-methanol solution (FUJIFILM Wako Pure chemical) for 20 min and stained with Azur-eosin-Methylene blue solution (Muto pure chemicals Co. Ltd, Tokyo, Japan) to visualize the cell fusion. Images were acquired using a KEYENCE／BZ-X800 microscope (Keyence Corporation, Osaka, Japan).

Treatment of pan-caspase inhibitors

Vero E6 cells were inoculated with rGn/Gc/L, rL and recombinant parental strain (rYG1) in a serial dilution and three days post-inoculation, media were replaced with fresh media containing 50 µM of caspase inhibitor, Z-VAD-FMK (Selleck chemicals, TX, USA). Dimethyl sulfoxide, DMSO (Sigma-Aldrich) was used as the diluent of pan-caspase inhibitor. Mock-infected Vero E6 cells were used as the experiment's controls. After 5 days-post virus inoculation cells were fixed with Mildform and stained with Azur-eosin-Methylene blue solution for visualization.

Western blotting

The recombinant viruses: rL, rGn/Gc/L and rYG1 were inoculated into Vero E6 cells at $1x10^3$ PFU/mL. One- and four-days post infection the cells were harvested, and lysate was prepared as explained in the chapter 1. Furthermore, Vero E6 cells were stimulated with 500 ng/µL of Actinomycin D (Sigma-Aldrich). Two days post stimulation cells were harvested, and the cell lysate to use as the positive control for apoptosis.

The lysates (15 μL) were loaded onto an SDS PAGE gel (e-PAGEL 1020 L, Atto, Tokyo, Japan). Followed by the electrophoresis, samples were electro blotted onto a 0.45 μm pore immunoblot PVDF membrane (Millipore, Billerica, MA, USA). The M protein of VSV was detected using anti-VSV M monoclonal antibody (kindly provided by Prof. Ayato Takada, Hokkaido University).

The lysates of Actinomycin D and recombinant viruses were incubated with anti-caspase1 antibody (Abcam, Cambridge, UK), PARP antibody (Cell Signaling, Danvers, MA, USA), NLRP3 (D2P5E) monoclonal antibody (Cell Signaling, MA, USA), anti-IL-1 beta multiclonal antibody (Abcam), anti-caspase3 antibody (Sigma-Aldrich) and anti-IL-1beta mAb (Abcam) in Can Get Signal Immunoreaction Enhancer Solution 1(Toyobo) were used as the primary antibodies and was incubated for 1 h at room temperature. Horseradish peroxidase-conjugated mouse anti-rabbit IgG (Jackson ImmunoResearch Laboratories Inc., Baltimore, MD, USA), diluted 10,000 times with Can Get Signal Immunoreaction Enhancer Solution 2 (Toyobo) was used as the secondary antibody and incubated for 1 h at room temperature. Bound antibodies were reacted with Amersham ECL Prime (GE Healthcare Life Science, PA, USA) and detected using an ImageQuant LAS 4000 mini (GE Healthcare Life Science). HRP-conjugated anti-GAPDH antibody (Proteintech, Rosemont, IL, USA) was used as the housekeeping-gene.

Co-infection of recombinant viruses

The recombinant virus; rYG1 was inoculated into Vero E6 cells at MOI 0.02 together with rGn, rGc or rL (ratios of 10:1,1:1,0.1:1) in a monolayered 6-well plate (Greiner Bio-One Co., Tokyo, Japan). Single infections of rYG1, rGn, rGc or rL were performed as controls. Eight days after inoculation, culture supernatant was collected and centrifuged to remove cells. Total RNA was extracted from culture supernatant by Isogen LS (Nippon Gene) according to

the manufacturer's instructions and cDNA was produced by ReverTra Ace cDNA synthesis kit (Nippon Genetics Co., Ltd, Tokyo, Japan). To know the virus of dominance in each fraction, three sites 804-1325 and 1792-2381 of M genome and 5135- 5883 of L genome were amplified by PCR. Purified PCR products were sequenced using a BigDye Terminator v3.1 Cycle Sequencing Kit (Applied Biosystems; Thermo Fisher Scientific) and Genetic Analyzer 3130 and Ligation Sequencing Kit (SQK-LSK109, Oxford Nanopore Technologies, UK), Native Barcoding Expansion 1-12 (EXP-NBD104, Oxford Nanopore Technologies and MinION Flowcell R9.4.1 (Oxford Nanopore Technologies). The real-time base-calling was done for raw fast5 signal data using Guppy v.4.3.4, released with MinKNOW software.

Apoptosis induction in rYG1-infected cells

The monolayer of Vero E6, Huh-7 and BHK/T7-9 cells were infected with rYG1 in a gradient of dilution. Soon after the infection, cells were stimulated by Actinomycin D (Sigma-Aldrich) in high to low concentrations (500, 400, 300, 200, 100 ng/µL). In addition, the rYG1 infection and Actinomycin D stimulation alone were used as controls. After three days of incubation, cells were fixed and stained as described above.

Results

Establishment of recombinant viruses using a reverse genetics system

I established a reverse genetics system for the SFTSV-YG1 strain, and seven different recombinant viruses of original YG1 with single, double, or triple mutations were rescued. Together with helper plasmids, as shown in Table 2, the transcription plasmids were transfected into BSR-T7/5 cells in a 60 mm culture dish. The supernatant was harvested after five days of incubation, and the Passage 1 (P1) virus was obtained. P1 virus was inoculated into Vero E6 cells for expansion and obtained P2 virus after 7-9 dpi. The rescued viruses are designated as rGn, rGc, rL, rGn/L, rGc/L, rGn/Gc, rGn/Gc/L, or rYG1 depending on bearing mutation(s) (Table 2). The genome detection of P2 viruses were carried out by RT-PCR and the viral proteins expression by IFA (data not shown). P2 virus were passages into Vero E6 cells and obtained P3 virus, which is used for downstream analysis as seed virus. Nucleotide sequences of all recombinant viruses were determined and confirmed using MinION and Sanger sequencing that there are no unnecessary mutations (Data not shown).

Plaque-forming activity and virus spread of recombinant viruses

The plaque-forming assay was performed using rescued viruses. The plaques formed by each recombinant virus were counted at 10 dpi and calculated the virus titer. All the recombinant viruses other than rGn/Gc/L showed virus titers higher than 6 x10^5 plaque-forming units (PFU)/mL (Figure 6A). The plaques formed by the recombinant viruses revealed different phenotypes depending on the mutations included in the virus. Plaques of rGn/Gc and rGn/Gc/L were similar in size to the original A4 (mutation in Gn/Gc) and B7 (mutations in Gn/Gc/L) subclones mentioned in Nishio *et al*., 2017. The viral plaques caused by rGn have a clear and large appearance, whereas the plaques of rGc also have a large but smoky appearance. In contrast, the plaques of rL were small and had a pinprick appearance. The

double mutant recombinant virus: rGn/L showed large, clear plaques with well-defined borders, similar to but more prominent than rGn. On the other hand, the plaques formed by rGc/L revealed a mixed phenotype of rL and rGc; they can be described as large plaques with a pinprick appearance (Figure 6B). These findings indicate that the virus cell-to-cell infection and its efficiency might differ depending on each recombinant virus's mutations. To examine the efficacy of virus cell entry, I generated the pseudotyped viruses bearing the YG1-GP-Y/R, GP-H/R, GPR, GP-Y/W, or GP-H/W, infecting the Vero E6 cells and measured the luciferase activity. The RLU of VSVΔG*- GP-H/W was significantly higher than the VSVΔG*- GP-Y/R, indicating that having two mutations (Y328H and R624W) in GP facilitates the cell entry than the wild type. In contrast, the only Y328H mutation in GP discourages cell entry which explains the lowest RLU of VSVΔG*- GP-H/R (Figure 7). The mutation in Gc alone, VSVΔG*- GP-Y/W, didn't show any significant difference meaning that the mutation R624W does not have a particular effect on viral entry alone.

A)

Virus	Genome Gn/Gc/L	Titer (PFU/mL)
rGn	H/R/N	1.8×10^6
rGc	Y/W/N	1.3×10^7
rL	Y/R/K	9.0×10^6
rGn/L	H/R/K	1.2×10^6
rGc/L	Y/W/K	1.5×10^7
rGn/Gc	H/W/N	6.0×10^6
rGn/Gc/L	H/W/K	2.8×10^4
rYG1	Y/R/N	2.2×10^6

B)

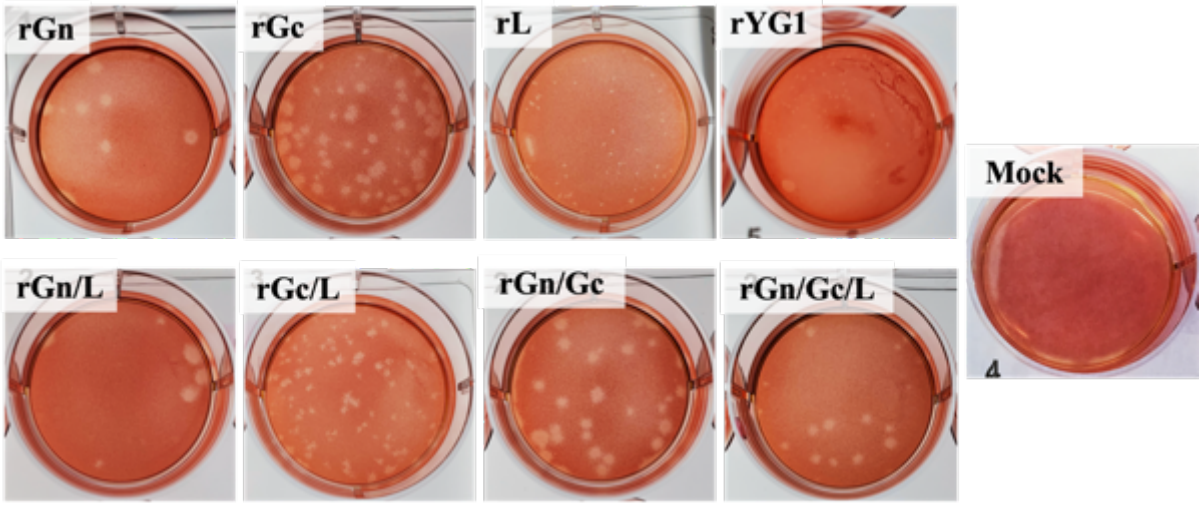

Figure 7. Virus titration and plaque-forming activity of recombinant viruses

A) Recombinant viruses and their titers of working stock.
B) The plaques of recombinant viruses. Photos were taken on 10 days after infection, it was 3 days after overlay of neutral red, except for rGc and rGn/Gc/L, which were taken on 9 days after infection.

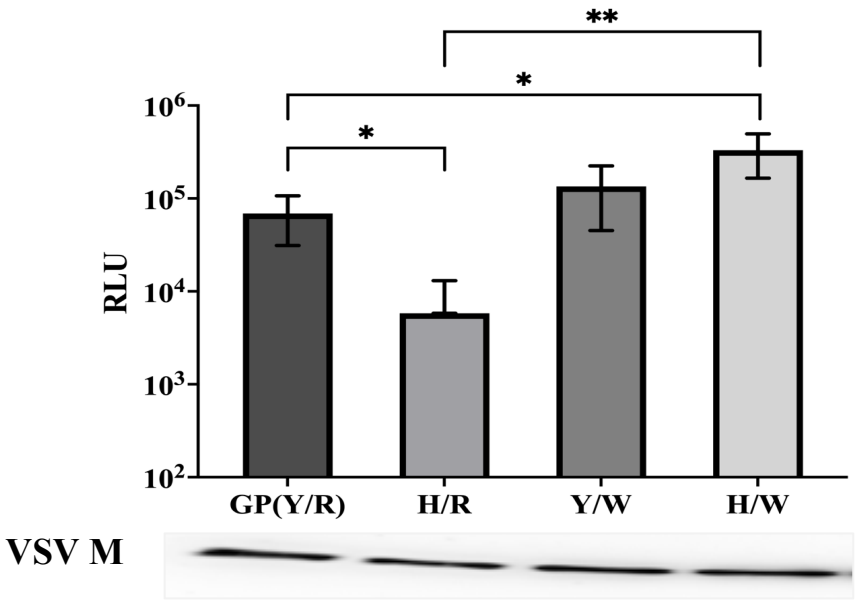

Figure 8. Comparison of viral entry using pseudotype viruses bearing YG1-GP with single/ double mutations.

Assessment of low pH-dependent cell fusion activity and CPE of recombinant viruses. In a previous study it showed the mutation in R624W in Gc induced strong syncytia formation in low pH condition and subclone B7 only demonstrated strong CPE in infected cells[9]. Therefore, cell fusion assay was carried out in this study, to demonstrate the fusion ability of the recombinant viruses. The recombinant virus, rGc, showed strong syncytia formation in low but not in neutral pH conditions. The rGn showed weaker cell fusion activity compared to rGc in low pH conditions. In contrast, rL showed intense CPE in low and normal pH conditions but no cell fusion activity (Figure 9). Both double mutant viruses, rGn/L, and rGc/L, showed intense CPE and cell fusion activity. Still, the robust CPE made it challenging to see the low pH-dependent cell fusion activity due to the detachment of cells (Figure 9). These data suggest that mutation in L (N1891K) might be essential in inducing CPE, whereas mutation in Gc (R624W) in cell fusion activity.

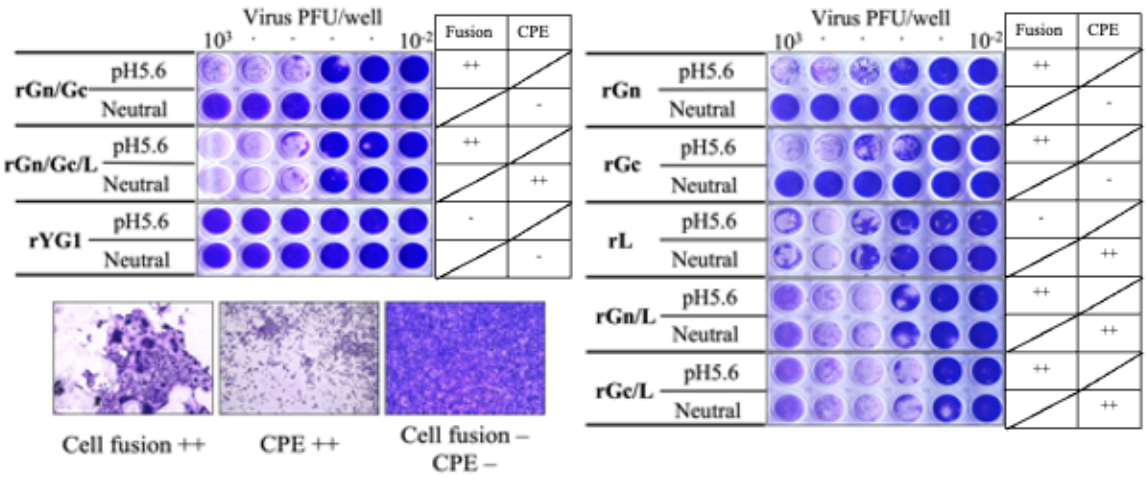

Figure 9. Assessment of low pH-dependent cell fusion activity and CPE of recombinant viruses.

Vero E6 cells were infected with serial dilutions of each recombinant virus and incubated for 7 days at 37ºC. The medium was replaced with 50 mM acetate-buffered saline with pH 5.6 and incubated for 2 min at room temperature. Then acetate buffer was replaced with fresh growth medium and incubated for 24 hours at 37ºC. The upper panel of each virus shows the lower pH (pH 5.6), and the lower panel shows the neutral pH. Representative images were shown below for cell fusion (++), CPE (++), cell fusion, and CPE (-).

Categorization of cell death induced by rL infection in Vero E6 cells

To analyze the cell death mechanism induced by the viral infection, I used the pan-caspaseinhibitor Z-VAD-FMK with the rGn/Gc/L, rL and rYG1- infected cells. The rYG1 which is not causing CPE, was used as the negative control. The Z-VAD-FMK inhibited the cell death induced by rGn/Gc/L and rL infection compared to the infected cells without inhibitors, indicating that the cell death caused by rGn/Gc/L and rL is a caspase-dependent cell death (Figure 10).

Actinomycin D and the quantity of cleaved PARP used as a positive control for apoptosis and Actinomycin D as negative control for pyroptosis. The cleavage of PARP was not prominent, in the infection of rL and rGn/Gc/L in both time durations (1 and 4 dpi) which did not show any difference compared to the mock-infected (Figure 11A). The programmed cell death induced by rL or rGn/Gc/L infection might not be due to apoptosis but due to another mechanism.

Furthermore, the bands were observed with anti-caspase 1 and 3 antibodies in both CPE-inducing viruses (rL, rGn/Gc/L) and non-CPE-inducing virus (rYG1) in 4 dpi but not in 1 dpi (Figure 11B). The pyroptosis cell death markers, caspase 1 and 3, were induced by the infection of rGn/Gc/L and rL, indicating that mutation in L (N1891K) caused the caspase-dependent cell death (Figure 11B and C). Interestingly, caspases 1 and 3 were expressed in rYG1- infected Vero E6 cells, indicating that wild-type virus infection can also induce the programmed cell death-related molecules (Figure 11B and C). The cell death caused by rGn/Gc/L and rL infection did not induce the release of the pro-inflammatory cytokine, IL-1beta, nor NLRP-3 inflammasome (Figure 11D and E). This result indicates that both CPE-inducing and non-inducing viruses induced caspase-related- programmed cell death, but not defined as pyroptosis. Despite the induction of caspase 1, CPE was caused only by viruses

with an 1891K alteration in the L genome segment. It is thought that non-CPE-inducing viruses also might suppress cell death after caspase 1 induction.

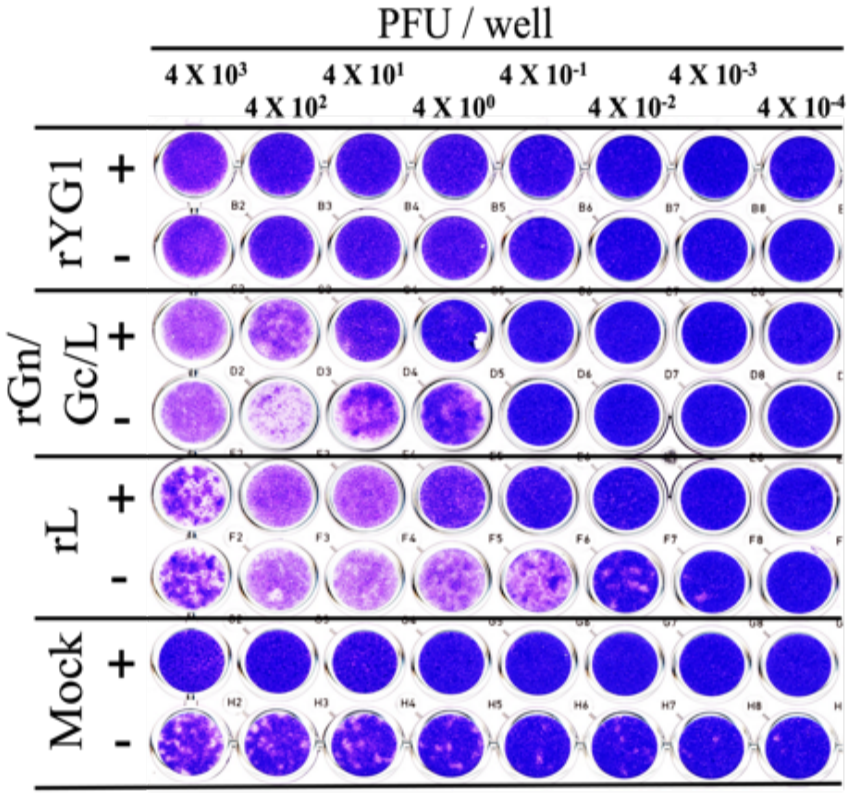

Figure 10. Inhibitory effects of pan-caspase inhibitor on CPE induced by recombinant SFTSV viruses.

Vero E6 cells were inoculated with recombinant viruses and three days post-inoculation, media were replaced with fresh media containing 50 μM of caspase inhibitor, Z-VAD-FMK in dimethyl sulfoxide (+) or dimethyl sulfoxide (-). Mock-infected Vero E6 cells were used as the experiment's controls. After 5 days-post inoculation cells were fixed and stained.

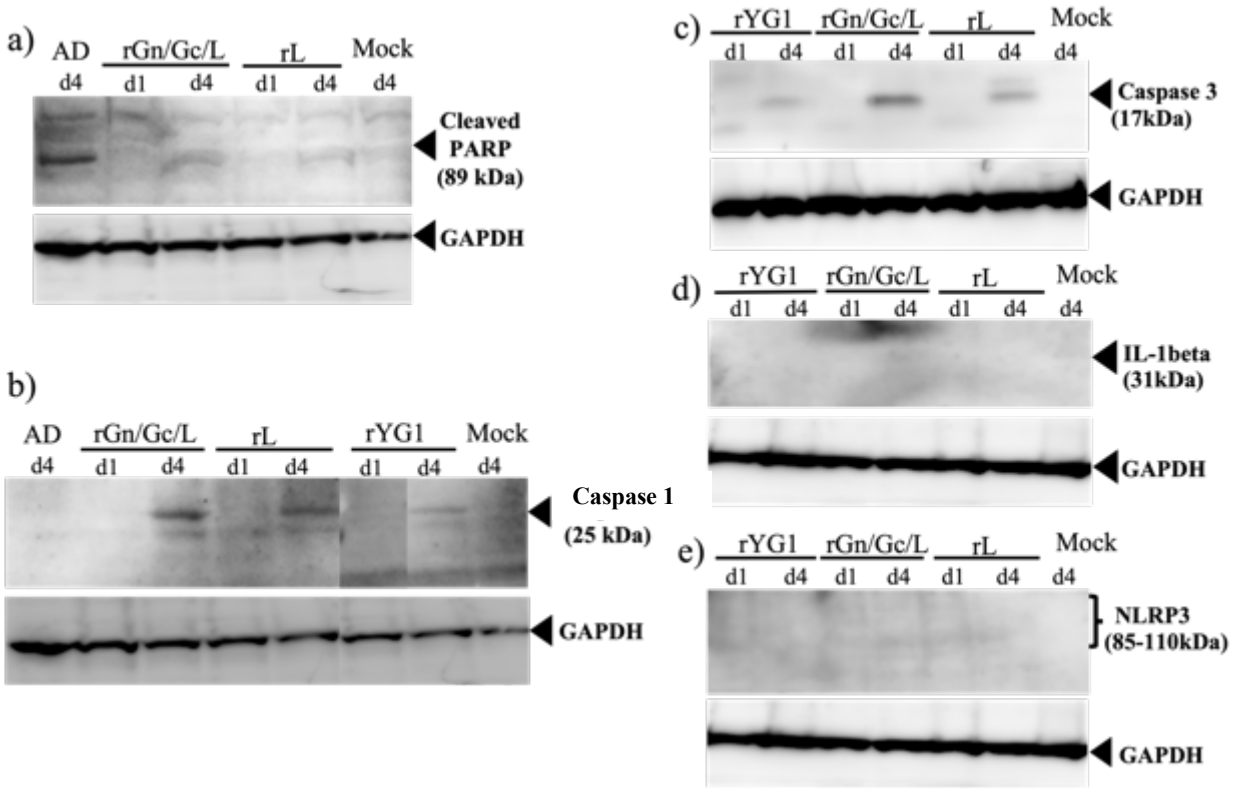

Figure 11. Induction of anti-caspase 1, anti-caspase 3, cleaved PARP, IL-1 beta and NLRP3 in SFTSV infected Vero E6 cells.
The recombinant viruses: rL, rGn/Gc/L and rYG1 were inoculated into Vero E6 cells at $1x10^3$ PFU/ml. One- and four-days post infection (d1 and d4) the cells were harvested, and lysates were prepared. Vero E6 cells were treated with 500ng/ µL of Actinomycin D (AD). Two-days post stimulation cells were harvested and prepared the cell lysate to use as the positive control for apoptosis. The lysates of Actinomycin D and recombinant viruses were incubated with PARP antibody, anti-caspase 1 antibody, anti-caspase 3 antibody, anti-IL-1 beta monoclonal antibody, and NLRP3 (D2P5E) monoclonal antibody as the primary antibodies. Horseradish peroxidase-conjugated mouse anti-rabbit IgG was used as the secondary antibody. HRP-conjugated anti-GAPDH antibody was used to adjust the total protein concentration in the lysate. Mock- infected cells were shown as SFTSV (-).

The impact of non-CPE-inducing viruses on CPE inducing viruses and Actinomycin D

Next, the impact of the non-CPE-inducing virus, rYG1 infection, on cell death by apoptosis induced by Actinomycin D was examined. The rYG1 infection alone didn't show any signs of CPE, in contrast to Actinomycin D stimulated Vero E6 cells which showed a high grade of cell death in all concentrations used in this study. The Vero E6 cells stimulated with Actinomycin D and infected with rYG1 showed cell death inhibition compared to those stimulated with Actinomycin D alone. As the Actinomycin D concentrations decreased, cell death suppression by rYG1 was increased independent of its dilution (Figure 12A). Furthermore, I used BHK-T7/9 and Huh-7 cells for the rYG1 infection to see the effect of the cell lines on cell death suppression. Similarly, BHK-T7/9 and Huh-7 infected rYG1 suppressed the cell death caused by Actinomycin D (Figure 12B and C).

The impact of parental virus on growth of rGn, rGc and rL viruses

The rYG1 could suppress the chemically induced cell death, and it might be able to suppress the cell death caused by the virus. Therefore, co-infection experiments were conducted to understand the virus competition *in vitro*. The rL infection showed apparent CPE, whereas rYG1 did not show CPE. No CPE was observed with co-infection of the rYG1 with rL even in 1:10 (data not shown). As shown in Table 3, the rL virus competed and was defeated by ten times lower amounts of rYG1. Characteristics causing CPE might not be advantage for the virus surviving. Similarly, both rGc and rGn viruses have also contested with rYG1, dominated by a ten times lower amount of rYG1(Table 3). These results indicate that rL, rGc, and rGn infection were suppressed and dominated by the parental virus rYG1 co-infection.

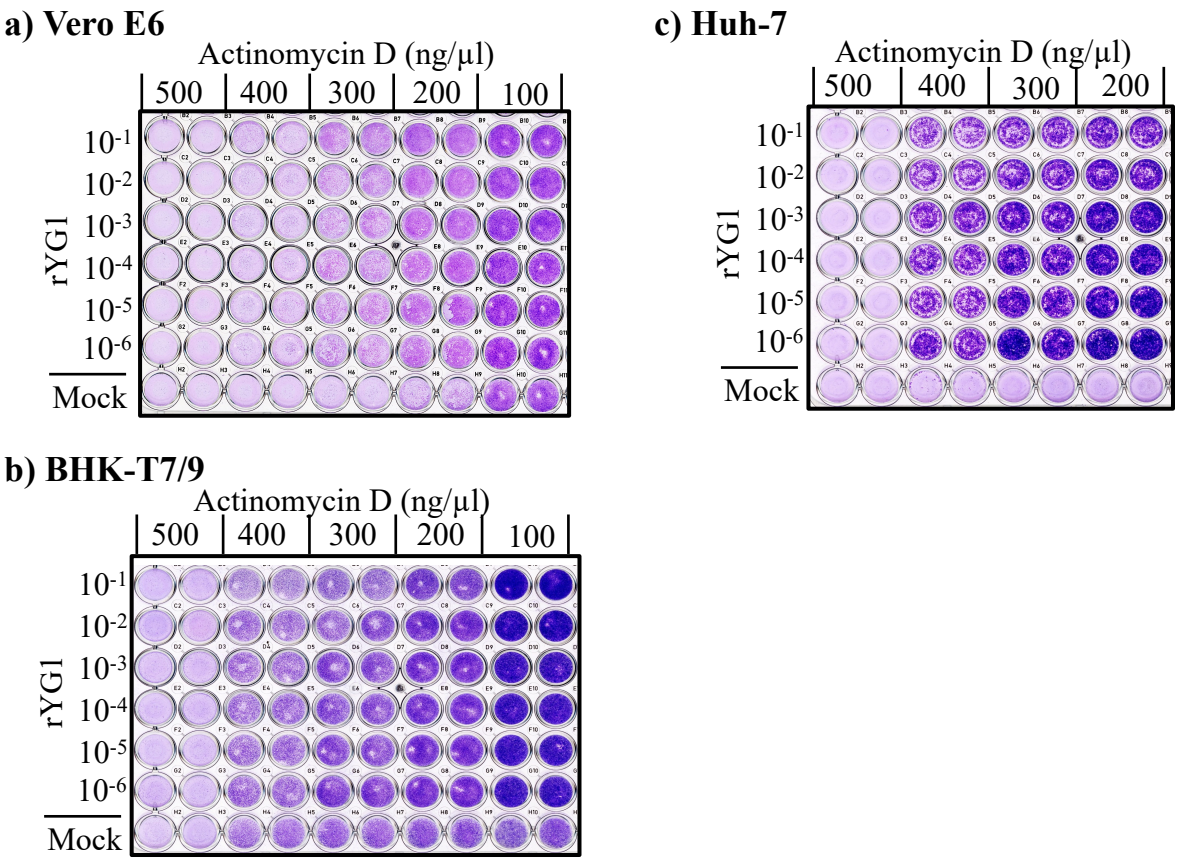

Figure 12: The impact of recombinant SFTSVs on Actinomycin D induced cell death in line cells, Vero E6, BHK-T7/9 and Huh-7 cells.

The monolayer of rYG1 inoculated Vero E6 (a), Huh7 (c) and BHK-T7/9 (b) cells in a gradient of dilution was cultured with Actinomycin D in various concentrations (500, 400, 300, 200, 100 ng/µL) and cells were fixed and stained after 7 days on incubation.

Table 3. Dominant growth of the parental virus in mixed infection

	Virus competitor	Sequence position	Ratio of competitors vs rYG1			
			10:1	**1:1**	**0.1:1**	**0:1**
rYG1 vs	**None**	-	rYG1	rYG1	rYG1	No virus
	rGn	1000	rYG1 > rGn	rYG1	rYG1	rGn
	rGc	1888	rYG1 = rGc	rYG1	rYG1	rGc
	rL	5689	rYG1 = rL	rYG1	rYG1	rL

The recombinant virus; rYG1 was inoculated into Vero E6 cells at moi 0.02 together with rGn, rGc or rL (ratios of 10:1, 1:1, 0.1:1). Single conditions of rYG1, rGn, rGc or rL were performed as controls.

Discussion

SFTS is an emerging disease with a high fatality rate caused by a member of the *phlebovirus* genus, which has become a significant health concern in most Asian countries due to the lack of therapeutics and pathological knowledge. Understanding the SFTSV life cycle in infected cells can shed light on the pathogenicity of the virus, which can fill the gaps in therapeutic development.

Yoshikawa *et al.* compared the sequence of isolated YG1 virus and the sequence in patient blood before isolation by next-generation sequencing. According to the results, viruses with Gn mutation (Y328H) account for approximately 30% of the patient blood[51](Table 1). However, no advantage was found in rGn virus propagation in Vero E6 cells. On the other hand, Gc mutation (R624W) was not detected in the patient blood[51]. Therefore, the Gn mutation would be disappeared during passage in Vero E6 cells. It is presumed that Gc mutation was acquired to compensate for the disadvantage of Gn mutation in the cloning process by limiting dilution using Vero E6 cells because the efficiency of rGn virus entry into Vero E6 cells restores by adding the Gc mutation.

Our previous findings show that the amino acid at position 624 in Gc of the original YG1 strain of SFTSV played an essential role in low-pH-dependent cell fusion activity[11]. Also, the polarity of amino acid position 1891 in the L segment of YG1 is critical for the polymerase activity and the L-segment C-terminal domain for genome transcription and viral replication[25]. Previous studies could not demonstrate the changes in properties brought by alteration of the amino acid substitution at position 328 in Gn.

By using recombinant viruses, the characteristics of each substitution were demonstrated. The viral plaques caused by rGn were larger than those of rL, meaning that the Y328H mutation in Gn showed a higher spread of infection. SFTSV Gn binds to nonmuscle myosin heavy

chain IIA (NMMHC-IIA), which is critical for the cellular entry of SFTSV[55]. In addition, the Gn likely contributes to receptor binding according to its position on the viral surface[56].

According to the fusion assay, the rGc virus with a single substitution of R624W showed more robust syncytia formation than rGn. This result indicates that R624W is an enhancer of fusion ability demonstrated by the Gc portion of SFTSV. A recent study has shown that phlebovirus Gc has played a vital role in the fusion process. The Gc structure of RVFV is similar to the class II fusion protein architecture, which identifies as the effector of membrane fusion[57].

The plaque size of viruses with L mutation (N1891K) altogether with mutation Y328H and/or R624W were enlarged, as shown in subclone B7[9]. In the region of plaque, cells were dead by CPE. A recent study suggested that during the SFTSV infection, it activates the NLPR3 inflammasome and pyroptosis, leading to IL-1β/IL-18 secretion[58]. In this study, the pan-caspaseinhibitor: Z-VAD-FMK could inhibit the cell death induced by L mutation (N1891K), indicating a caspase-dependent mechanism. However, Caspase1 and Caspase3, markers of apoptosis and pyroptosis, were found to be induced even in wild-type viruses that did not show CPE. Perhaps only rL viruses fail to block cell death after the appearance of caspases. Consistent with the above observation, rYG1 was found to suppress actinomycin D-induced cell death.

Competitive infection experiments showed that the parental strain rYG1 grew dominantly against three viruses with single mutations, Y328H and R624W in GP and N1891K in L protein. Y328H was the dominant quasispecies in blood, but in vitro, competitive assay in Vero E6 cells, it was not advantageous for survival. Because after the isolation of the YG1 virus by Vero E6 cells, the population of Y328H was reduced in the previous report[51]. The Y328H substitution seemed to be advantageous to cell-to-cell infection. Y328H may favor

growth in cells elsewhere in vivo rather than Vero cells. B lymphocytes and macrophages are thought to play essential roles in developing virulence[50]. In this study, we generated a single mutant virus, rGn. It is possible to determine the target cells *in vivo* using the rGn.

Not inducing cell death is considered advantageous for the virus's continuous propagation and persistent infection. Furthermore, continued stimulation of the immune system may contribute to virulence development. Detailed research on the relationship between cell death suppression and pathogenicity warrants future studies.

Brief Summary

YG1 strain is the first isolated SFTSV strain in Japan. Previously, our research team identified three amino acid variations from isolated viruses through limiting dilution assay. One variation on Gn (Y328H) was the major population among patient blood. Other variations on Gc (R624W) and L (N1891K) were under detection in patient blood but affected low-pH-dependent cell fusion activity, polymerase activity, and cytopathic effect (CPE). However, a virus with every substitution was not found, and the role of individual mutations in quasispecies was still unclear. I generated viruses with specific mutations in this study to elucidate their involvement in viral infectivity, cell fusion activity, and cell death. I rescued viruses with 1 to 3 mutations of Y328H, R624W on GP, N1891K on L protein, and a virus with the gene sequence of the YG1 subclones. The plaque formation, cell fusion, CPE, and cell death of recombinant viruses were analyzed. Mutations Y328H and R624W on the GP alone increased the cell fusion ability, but the effect was more substantial with R624W. Y328H on the GP was found to increase plaque size. The enhancing effect was even more pronounced with both Y328H and R624W. Pseudotyped VSV of Y328H and R624W mutations also showed higher entry to Vero E6 cells. Viruses with the N1891K mutation on L alone (rL) exhibited significant CPE with pinhole-sized plaques, whereas both GP mutations did not induce CPE.

CPE induced by rL was inhibited by pan-caspase inhibitor Z-VAD-FMK. Surprisingly, I found that these programmed death-related molecules, caspase 1 and caspase 3, were also influenced by wild-type virus infection. These results indicated that N1891K mutations were involved in cell death caused by programmed cell death. Furthermore, parental virus rYG1 showed suppression of Actinomycin D-induced cell death. The rL virus competed and was defeated by ten times lower amounts of the parental virus. Despite high polymerase activity, N1891K mutation on L was not advantageous for virus survival. Although the N1891K

mutation is disadvantageous for survival, it is thought that viruses with both Gn and Gc mutations survived and were detected as CPE-inducing viruses. This result suggests that combining mutations may increase mutant viruses' viability, leading to new pathogenic viruses' appearance.

Conclusion

The SFTS is widely distributed in East Asian countries, including China, Japan, South Korea, Vietnam, and Taiwan. In Japan, SFTS is endemic to southern parts of the country, and ticks, including *Haemaohysalis longicornis* and *Amblyomma testudinarium*, are the vectors. Therefore, the people engaged in farming and animal activities are the risk factors for SFTS. The SFTS has been investigated for over a decade in Japan and other East Asian countries; there are no effective measures to control the spread of the infection. However, due to the same, SFTS cases and epidemic regions has been skyrocketed due to the unavailability of antiviral drugs and vaccines. However, the molecular mechanism has yet to be elucidated entirely in SFTSV, which is vital to produce antivirals for the disease.

This study aims to provide relevant information on the SFTSV life cycle and its molecular mechanism, which will be helpful in the control of SFTS in Asian countries.

The subcellular localization of the viral proteins broadens the understanding of the SFTSV life cycle, which helps find antiviral targets for vaccine development. Also, the information on the role of cellular compartments aids future researchers in apprehending the virus assembly and, subsequently, the formation of progeny viruses.

The reverse genetics system of viruses has transformed the field of interest in so many research laboratories worldwide, and it has provided vital insights into the replication and pathogenesis of RNA viruses. I succeeded in introducing the reverse genetic system to SFTSV despite the difficulties in isolating the mutants of the YG1 strain. The studies of YG1 mutants became possible through reverse genetics, which can illustrate the significant virological properties and their differences among YG1 quasispecies. Interestingly, this study made it possible to understand that virus selection, suppression, and pathogenesis work hand in hand to get the best outcome of the virus infection among subclones of the same virus population. The viral signatures of networks interact differently with viral genes in different

cell lines. In vitro studies using different cell lines under diverse conditions precisely mimic the in vivo environment inside the organism. This allowed us to understand the interplay of microbial communities and host cells within an entire organism. The information gathered in this study helps identify cellular genes associated with disease risk and therefore predict which human or animal hosts should be vaccinated or prophylaxed. Understanding the pathogenesis of SFTSV isn't sufficient because all viruses create mutations to resist antiviral targets, and it is a challenging task to give a permanent solution to zoonotic diseases caused by viral infections. Therefore, the knowledge of the pathogenesis of SFTSV allows us to evaluate various intervention strategies aimed at mitigating the risk of transmission of SFTSV by having a holistic approach to connect and communicate to solve the emerging/re-emerging viral diseases in the future, as suggested by One Health approach.

Acknowledgement

Foremost, I would like to express my sincere gratitude to my supervisor Associate Professor Kumiko Yoshimatsu, Laboratory of Animal Experiment, Institute for Genetic Medicine, Hokkaido University, Japan, for the continuous support of my scientific research work, the well-being of me and my entire family and every other relevant aspect is immeasurable to achieve this work.

I am grateful to my vice-supervisor, Lecturer Yoshimi Tsuda, for her kind guidance and support in uplifting my technical, scientific, and intellectual capacity during my postgraduate studies. Besides my supervisors, my sincere gratitude goes to Professor Jiro Arikawa for his guidance and thoughtful advice throughout my career. My sincere thanks also go to Assistant Professor Kenta Shimizu for accommodating me in his busy schedule to help me with my research and providing valuable comments and technical support. All of them were previously in the Laboratory of Microbiology and Infectious Diseases, Faculty of Medicine, Hokkaido University, Japan.

Special gratitude goes to my research advisors, Professor Hiroaki Kariwa, Laboratory of Public Health, Faculty of Veterinary Medicine, Hokkaido University, Japan; Professor Chie Nakajima, Division of Bioresources, International Institute for Zoonosis Control (IIZC), Hokkaido University, Japan; Associate Professor, Masashi Shingai, Division of Biologics Development, IIZC, Hokkaido University and Associate Professor Keita Matsuno, Division of Risk Analysis and Management, IIZC, Hokkaido University, Japan. Their guidance and constructive comments were very important for the improvement of the quality of this study.

I am particularly grateful for the continuous support, warm encouragement, and constructive comments from my colleague Dr. Devinda Muthusinghe, previously Laboratory of Animal Experiment, Institute for Genetic Medicine, Hokkaido University, Japan, throughout my

career. I thank my fellow lab members from the Laboratory of Animal Experiment, IGM, Wei Xhuoxing and Emmanuel Kodua, and past members of the Laboratory of Microbiology and Infectious Diseases, Faculty of Medicine, Hokkaido University, Japan, for the stimulating discussions and for all the fun Ihave had together as a team. Many thanks to the technical staff members, Mr. Hiroyuki Murota and Mr. Koki Otaki of the Laboratory of Animal Experiment, Institute for Genetic Medicine, Hokkaido University, Japan, for their continuous support in technical work.

This study was made possible through the financial support received by the Japanese government (MONBUKAGAKUSHO: MEXT) postgraduate research scholarship program offered by the Ministry of Education, Culture, Sports, Science, and Technology.

Last but not least, I would like to express my deepest gratitude to my husband and my daughter, for their sacrifice, love, and support; my parents for giving birth to me in the first place and supporting me by all means throughout my life; and my brother for his love and support.

References

1 Yokomizo, K., Tomozane, M., Sano, C. & Ohta, R. Clinical Presentation and Mortality of Severe Fever with Thrombocytopenia Syndrome in Japan: A Systematic Review of Case Reports. *Int J Environ Res Public Health* **19**, doi:10.3390/ijerph19042271 (2022).

2 Yu, X. J. *et al.* Fever with thrombocytopenia associated with a novel bunyavirus in China. *N Engl J Med* **364**, 1523-1532, doi:10.1056/NEJMoa1010095 (2011).

3 Ryu, B. H. *et al.* Extensive severe fever with thrombocytopenia syndrome virus contamination in surrounding environment in patient rooms. *Clin Microbiol Infect* **24**, 911.e911-911.e914, doi:10.1016/j.cmi.2018.01.005 (2018).

4 Chen, C. *et al.* Animals as amplification hosts in the spread of severe fever with thrombocytopenia syndrome virus: A systematic review and meta-analysis. *Int J Infect Dis* **79**, 77-84, doi:10.1016/j.ijid.2018.11.017 (2019).

5 Takahashi, T. *et al.* The first identification and retrospective study of Severe Fever with Thrombocytopenia Syndrome in Japan. *J Infect Dis* **209**, 816-827, doi:10.1093/infdis/jit603 (2014).

6 Liu, Q., He, B., Huang, S. Y., Wei, F. & Zhu, X. Q. Severe fever with thrombocytopenia syndrome, an emerging tick-borne zoonosis. *Lancet Infect Dis* **14**, 763-772, doi:10.1016/S1473-3099(14)70718-2 (2014).

7 Filone, C. M., Heise, M., Doms, R. W. & Bertolotti-Ciarlet, A. Development and characterization of a Rift Valley fever virus cell-cell fusion assay using alphavirus replicon vectors. *Virology* **356**, 155-164, doi:10.1016/j.virol.2006.07.035 (2006).

8 Lozach, P. Y. *et al.* Entry of *bunyaviruses* into mammalian cells. *Cell Host Microbe* **7**, 488-499, doi:10.1016/j.chom.2010.05.007 (2010).

9 Nishio, S. *et al.* Establishment of Subclones of the Severe Fever with Thrombocytopenia Syndrome Virus YG1 Strain Selected Using Low pH-Dependent Cell Fusion Activity. *Jpn J Infect Dis* **70**, 388-393, doi:10.7883/yoken.JJID.2016.357 (2017).

10 Gwon, Y. D., Nematollahi Mahani, S. A., Nagaev, I., Mincheva-Nilsson, L. & Evander, M. Rift Valley Fever Virus Propagates in Human Villous Trophoblast Cell Lines and Induces Cytokine mRNA Responses Known to Provoke Miscarriage. *Viruses* **13**, doi:10.3390/v13112265 (2021).

11 Tsuda, Y. *et al.* The amino acid at position 624 in the glycoprotein of SFTSV (severe fever with thrombocytopenia virus) plays a critical role in low-pH-dependent cell fusion activity. *Biomed Res* **38**, 89-97, doi:10.2220/biomedres.38.89 (2017).

12 Xu, B. *et al.* Metagenomic analysis of fever, thrombocytopenia and leukopenia syndrome (FTLS) in Henan Province, China: discovery of a new bunyavirus. *PLoS Pathog* **7**, e1002369, doi:10.1371/journal.ppat.1002369 (2011).

13 Kim, K. H., Ko, M. K., Kim, N., Kim, H. H. & Yi, J. Seroprevalence of Severe Fever with Thrombocytopenia Syndrome in Southeastern Korea, 2015. *J Korean Med Sci* **32**, 29-32, doi:10.3346/jkms.2017.32.1.29 (2017).

14 Tran, X. C. *et al.* Endemic Severe Fever with Thrombocytopenia Syndrome, Vietnam. *Emerg Infect Dis* **25**, 1029-1031, doi:10.3201/eid2505.181463 (2019).

15 Wen, H. L. *et al.* Severe fever with thrombocytopenia syndrome, Shandong Province, China, 2011. *Emerg Infect Dis* **20**, 1-5, doi:10.3201/eid2001.120532 (2014).

16 Robles, N. J. C., Han, H. J., Park, S. J. & Choi, Y. K. Epidemiology of severe fever and thrombocytopenia syndrome virus infection and the need for therapeutics for the prevention. *Clin Exp Vaccine Res* **7**, 43-50, doi:10.7774/cevr.2018.7.1.43 (2018).

17 Kobayashi, Y. *et al.* Severe Fever with Thrombocytopenia Syndrome, Japan, 2013-2017. *Emerg Infect Dis* **26**, 692-699, doi:10.3201/eid2604.191011 (2020).

18 Plegge, T., Hofmann-Winkler, H., Spiegel, M. & Pöhlmann, S. Evidence that Processing of the Severe Fever with Thrombocytopenia Syndrome Virus Gn/Gc Polyprotein Is Critical for Viral Infectivity and Requires an Internal Gc Signal Peptide. *PLoS One* **11**, e0166013, doi:10.1371/journal.pone.0166013 (2016).

19 Hofmann, H. *et al.* Severe fever with thrombocytopenia virus glycoproteins are targeted by neutralizing antibodies and can use DC-SIGN as a receptor for pH-dependent entry into human and animal cell lines. *J Virol* **87**, 4384-4394, doi:10.1128/JVI.02628-12 (2013).

20 Zhou, H., Sun, Y., Guo, Y. & Lou, Z. Structural perspective on the formation of ribonucleoprotein complex in negative-sense single-stranded RNA viruses. *Trends Microbiol* **21**, 475-484, doi:10.1016/j.tim.2013.07.006 (2013).

21 Jäntti, J. *et al.* Immunocytochemical analysis of Uukuniemi virus budding compartments: role of the intermediate compartment and the Golgi stack in virus maturation. *J Virol* **71**, 1162-1172, doi:10.1128/JVI.71.2.1162-1172.1997 (1997).

22 Lundu, T. *et al.* Targeting of severe fever with thrombocytopenia syndrome virus structural proteins to the ERGIC (endoplasmic reticulum Golgi intermediate compartment) and Golgi complex. *Biomed Res* **39**, 27-38, doi:10.2220/biomedres.39.27 (2018).

23 Ito, N. *et al.* Improved recovery of rabies virus from cloned cDNA using a vaccinia virus-free reverse genetics system. *Microbiol Immunol* **47**, 613-617, doi:10.1111/j.1348-0421.2003.tb03424.x (2003).

24 Jiao, L. *et al.* Structure of severe fever with thrombocytopenia syndrome virus nucleocapsid protein in complex with suramin reveals therapeutic potential. *J Virol* **87**, 6829-6839, doi:10.1128/JVI.00672-13 (2013).

25 Noda, K. *et al.* The Polarity of an Amino Acid at Position 1891 of Severe Fever with Thrombocytopenia Syndrome Virus L Protein Is Critical for the Polymerase Activity. *Viruses* **13**, doi:10.3390/v13010033 (2020).

26 Schindelin, J. *et al.* Fiji: an open-source platform for biological-image analysis. *Nat Methods* **9**, 676-682, doi:10.1038/nmeth.2019 (2012).

27 Zinchuk, V., Zinchuk, O. & Okada, T. Quantitative colocalization analysis of multicolor confocal immunofluorescence microscopy images: pushing pixels to explore biological phenomena. *Acta Histochem Cytochem* **40**, 101-111, doi:10.1267/ahc.07002 (2007).

28 Ramanathan, H. N. *et al.* Dynein-dependent transport of the hantaan virus nucleocapsid protein to the endoplasmic reticulum-Golgi intermediate compartment. *J Virol* **81**, 8634-8647, doi:10.1128/JVI.00418-07 (2007).

29 Panda, D. *et al.* RNAi screening reveals requirement for host cell secretory pathway in infection by diverse families of negative-strand RNA viruses. *Proc Natl Acad Sci U S A* **108**, 19036-19041, doi:10.1073/pnas.1113643108 (2011).

30 Novoa, R. R., Calderita, G., Cabezas, P., Elliott, R. M. & Risco, C. Key Golgi factors for structural and functional maturation of bunyamwera virus. *J Virol* **79**, 10852-10863, doi:10.1128/JVI.79.17.10852-10863.2005 (2005).

31 Salanueva, I. J. *et al.* Polymorphism and structural maturation of bunyamwera virus in Golgi and post-Golgi compartments. *J Virol* **77**, 1368-1381, doi:10.1128/jvi.77.2.1368-1381.2003 (2003).

32 Albornoz, A., Hoffmann, A. B., Lozach, P. Y. & Tischler, N. D. Early Bunyavirus-Host Cell Interactions. *Viruses* **8**, doi:10.3390/v8050143 (2016).

33 Piper, M. E., Sorenson, D. R. & Gerrard, S. R. Efficient cellular release of Rift Valley fever virus requires genomic RNA. *PLoS One* **6**, e18070, doi:10.1371/journal.pone.0018070 (2011).

34 Shi, X., Lappin, D. F. & Elliott, R. M. Mapping the Golgi targeting and retention signal of Bunyamwera virus glycoproteins. *J Virol* **78**, 10793-10802, doi:10.1128/JVI.78.19.10793-10802.2004 (2004).

35 Lopez, N., Muller, R., Prehaud, C. & Bouloy, M. The L protein of Rift Valley fever virus can rescue viral ribonucleoproteins and transcribe synthetic genome-like RNA molecules. *J Virol* **69**, 3972-3979, doi:10.1128/JVI.69.7.3972-3979.1995 (1995).

36 Strandin, T., Hepojoki, J., Wang, H., Vaheri, A. & Lankinen, H. The cytoplasmic tail of hantavirus Gn glycoprotein interacts with RNA. *Virology* **418**, 12-20, doi:10.1016/j.virol.2011.06.030 (2011).

37 Strandin, T., Hepojoki, J. & Vaheri, A. Cytoplasmic tails of bunyavirus Gn glycoproteins-Could they act as matrix protein surrogates? *Virology* **437**, 73-80, doi:10.1016/j.virol.2013.01.001 (2013).

38 Snippe, M., Smeenk, L., Goldbach, R. & Kormelink, R. The cytoplasmic domain of tomato spotted wilt virus Gn glycoprotein is required for Golgi localisation and interaction with Gc. *Virology* **363**, 272-279, doi:10.1016/j.virol.2006.12.038 (2007).

39 Olal, D. *et al.* Structural insights into RNA encapsidation and helical assembly of the Toscana virus nucleoprotein. *Nucleic Acids Res* **42**, 6025-6037, doi:10.1093/nar/gku229 (2014).

40 Gerlach, P., Malet, H., Cusack, S. & Reguera, J. Structural Insights into Bunyavirus Replication and Its Regulation by the vRNA Promoter. *Cell* **161**, 1267-1279, doi:10.1016/j.cell.2015.05.006 (2015).

41 Muriaux, D. *et al.* Role of murine leukemia virus nucleocapsid protein in virus assembly. *J Virol* **78**, 12378-12385, doi:10.1128/JVI.78.22.12378-12385.2004 (2004).

42 Licata, J. M., Johnson, R. F., Han, Z. & Harty, R. N. Contribution of ebola virus glycoprotein, nucleoprotein, and VP24 to budding of VP40 virus-like particles. *J Virol* **78**, 7344-7351, doi:10.1128/JVI.78.14.7344-7351.2004 (2004).

43 Vennema, H. *et al.* Nucleocapsid-independent assembly of coronavirus-like particles by co-expression of viral envelope protein genes. *EMBO J* **15**, 2020-2028 (1996).

44 Swenson, D. L. *et al.* Generation of Marburg virus-like particles by co-expression of glycoprotein and matrix protein. *FEMS Immunol Med Microbiol* **40**, 27-31, doi:10.1016/S0928-8244(03)00273-6 (2004).

45 Overby, A. K., Pettersson, R. F. & Neve, E. P. The glycoprotein cytoplasmic tail of Uukuniemi virus (Bunyaviridae) interacts with ribonucleoproteins and is critical for genome packaging. *J Virol* **81**, 3198-3205, doi:10.1128/JVI.02655-06 (2007).

46 Brennan, B. *et al.* Reverse genetics system for severe fever with thrombocytopenia syndrome virus. *J Virol* **89**, 3026-3037, doi:10.1128/JVI.03432-14 (2015).

47 Tani, H. *et al.* Characterization of Glycoprotein-Mediated Entry of Severe Fever with Thrombocytopenia Syndrome Virus. *J Virol* **90**, 5292-5301, doi:10.1128/JVI.00110-16 (2016).

48 Tani, H. *et al.* Identification of the amino acid residue important for fusion of severe fever with thrombocytopenia syndrome virus glycoprotein. *Virology* **535**, 102-110, doi:10.1016/j.virol.2019.06.014 (2019).

49 Gao, C. *et al.* Nonstructural Protein NSs Activates Inflammasome and Pyroptosis through Interaction with NLRP3 in Human Microglial Cells Infected with Severe Fever with Thrombocytopenia Syndrome Bandavirus. *J Virol* **96**, e0016722, doi:10.1128/jvi.00167-22 (2022).

50 Suzuki, T. *et al.* Severe fever with thrombocytopenia syndrome virus targets B cells in lethal human infections. *J Clin Invest* **130**, 799-812, doi:10.1172/JCI129171 (2020).

51 Yoshikawa, T. *et al.* Phylogenetic and Geographic Relationships of Severe Fever With Thrombocytopenia Syndrome Virus in China, South Korea, and Japan. *J Infect Dis* **212**, 889-898, doi:10.1093/infdis/jiv144 (2015).

52 Shi, X. *et al.* Bunyamwera orthobunyavirus glycoprotein precursor is processed by cellular signal peptidase and signal peptide peptidase. *Proc Natl Acad Sci U S A* **113**, 8825-8830, doi:10.1073/pnas.1603364113 (2016).

53 Buchholz, U. J., Finke, S. & Conzelmann, K. K. Generation of bovine respiratory syncytial virus (BRSV) from cDNA: BRSV NS2 is not essential for virus replication in tissue culture, and the human RSV leader region acts as a functional BRSV genome promoter. *J Virol* **73**, 251-259, doi:10.1128/JVI.73.1.251-259.1999 (1999).

54 Johnson, K. N., Zeddam, J. L. & Ball, L. A. Characterization and construction of functional cDNA clones of Pariacoto virus, the first Alphanodavirus isolated outside Australasia. *J Virol* **74**, 5123-5132, doi:10.1128/jvi.74.11.5123-5132.2000 (2000).

55 Sun, Y. *et al.* Nonmuscle myosin heavy chain IIA is a critical factor contributing to the efficiency of early infection of severe fever with thrombocytopenia syndrome virus. *J Virol* **88**, 237-248, doi:10.1128/JVI.02141-13 (2014).

56 Wu, Y. *et al.* Structures of phlebovirus glycoprotein Gn and identification of a neutralizing antibody epitope. *Proc Natl Acad Sci U S A* **114**, E7564-E7573, doi:10.1073/pnas.1705176114 (2017).

57 Dessau, M. & Modis, Y. Crystal structure of glycoprotein C from Rift Valley fever virus. *Proc Natl Acad Sci U S A* **110**, 1696-1701, doi:10.1073/pnas.1217780110 (2013).

58 Li, Z. *et al.* Activation of the NLRP3 inflammasome and elevation of interleukin-1β secretion in infection by sever fever with thrombocytopenia syndrome virus. *Sci Rep* **12**, 2573, doi:10.1038/s41598-022-06229-0 (2022).